Journal of Coastal Research	35	2	269–286	Coconut Creek, Florida	March 2019

A 50-Year Sr/Ca Time Series from an Enclosed, Shallow-Water Guam Coral: *In situ* Monitoring and Extraction of a Temperature Trend, Annual Cycle, and ENSO and PDO Signals

www.cerf-jcr.org

Tomoko Bell[†‡], Mark A. Lander[‡], John W. Jenson[‡]*, Richard H. Randall[‡], Judson W. Partin[§], and Nancy G. Prouty[††]

[†]Atmosphere and Ocean Research Institute
University of Tokyo
Chiba, Japan

[‡]Water and Environmental Research Institute of the Western Pacific
University of Guam
Mangilao 96923, Guam

[§]Institute for Geophysics
Jackson School of Geosciences
University of Texas
Austin, TX 78705, U.S.A.

[††]USGS Pacific Coastal and Marine Science Center
Santa Cruz, CA 95060, U.S.A.

www.JCRonline.org

ABSTRACT

Bell, T.; Lander, M.A.; Jenson, J.W.; Randall, R.H.; Partin, J.W., and Prouty, N.G., 2019. A 50-year Sr/Ca time series from an enclosed, shallow-water Guam coral: *In situ* monitoring and extraction of a temperature trend, annual cycle, and ENSO and PDO signals. *Journal of Coastal Research,* 35(2), 269–286. Coconut Creek (Florida), ISSN 0749-0208.

Located on the northern edge of the West Pacific Warm Pool and having a developed economy and modern infrastructure, Guam is well positioned and equipped for obtaining natural records of the west Pacific maritime paleoclimate. This study was a proof of concept to explore whether useful climate proxy records might be obtained from coral at readily accessible, even if geochemically nonoptimal, coastal sites. A 50-year Sr/Ca record (1960–2010) was thus obtained from a shallow-water, near-shore *Porites lutea* colony at a recreational facility inside Guam's Apra Harbor and compared with local and regional meteorological records, including the El Niño–Southern Oscillation (ENSO) and Pacific Decadal Oscillation (PDO) indices. The accessibility of the site enabled documentation of relevant environmental variables for 16 months (September 2009–December 2010): seawater δ^{18}O, pH, seawater cations, and nitrate. Time series of seawater δ^{18}O, pH, and cations show evidence of freshwater input from direct rainfall and stream discharge into the harbor. An anomalously higher mean and variable concentrations of Ba suggest the presence of river-borne, fine-grained terrigenous sediment. Nevertheless, the Sr/Ca time series reproduces a long-term warming trend seen in historical records of local air temperature and regional sea-surface temperature (SST) and closely tracks the ENSO and PDO indices over the entire 50-year record. The consistency of the results with Guam's historical instrumental records, previous coral δ^{18}O results from Guam obtained by others, and previous Sr/Ca proxy results for SST in similar environments elsewhere demonstrate that accessible near-shore sites—where environmental conditions can be monitored—can produce useful Sr/Ca records of local and regional climate phenomena.

ADDITIONAL INDEX WORDS: *El Niño–Southern Oscillation, Pacific Decadal Oscillation,* Porites lutea*,* in situ *environmental monitoring of coral.*

INTRODUCTION

Guam's location in the tropical western North Pacific,[1] almost 3000 km from continental climatic influences (Figure 1a), along with its abundant coral reefs (USGS, 2016) and limestone caves containing speleothems (Partin *et al*., 2012; Sinclair *et al*., 2008, 2012; Taboroši, Jenson, and Mylroie, 2005), give it a unique potential as an informative source of maritime climate proxy data for the western North Pacific region. This region is of particular interest to studies of global climate because it includes the northern edge of the West Pacific Warm Pool (WPWP). With the highest open-ocean water temperatures in the world (>28°C; Yan *et al*., 1992) and its dynamic link to the El Niño–Southern Oscillation (ENSO), the WPWP is a central component of the global climate system. Accurate understanding of the climate history of this region is thus important for understanding global climate history and for the development of reliable models by which to forecast changes in global climate and effects on regional ecosystems, societies, and economies (Glantz, Katz and Nicholls, 1991). Local interest in the climatic history of Guam and nearby islands is driven by the acknowledged sensitivity of small-island freshwater resources to regional climatic variations, particularly the frequency, intensity, and durations of storms and droughts (Lander, 1994b).

Given Guam's developed economy and infrastructure, local researchers are well- equipped for coastal research, including studies of coral paleoclimate records. The study reported here

DOI: 10.2112/JCOASTRES-D-16-00099.1 received 31 May 2016; accepted in revision 16 December 2016; corrected proofs received 22 October 2018; published pre-print online 30 November 2018.
*Corresponding author: jjenson@triton.uog.edu

[1]By tropical western North Pacific, the authors mean the region around the Mariana Islands, SE to the Caroline Islands, south toward New Guinea, SW to Palau, west to the Philippines, NW to the Ryukyu Islands, and north to the Volcano Islands.

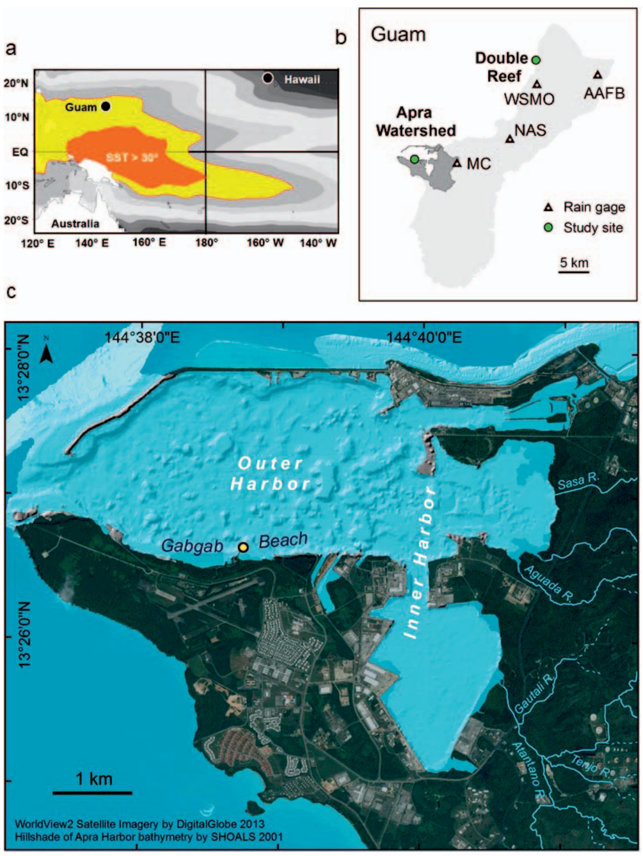

Figure 1. (a) Location of Guam in the western Pacific Ocean, and in the West Pacific Warm Pool (mean annual temperatures) (Sadler *et al.*, 1987). (b) Coral sampling sites on Guam: Gabgab Beach (this study) and Double Reef (Asami *et al.*, 2004, 2005). Apra Watershed, from which freshwater streams flow into Apra Harbor. Rain gages used in this study: AAFB, Anderson Air Force Base; WSMO, Weather Service Meteorological Station; GIAP, Guam International Airport; NAS, Naval Air Station; MC, Mount Chachao. (c) Apra Harbor bathymetry and detail, with location of study site. Streams entering from Apra Watershed are highlighted.

was a proof of concept to assess whether coral in readily accessible coastal locations might yield useful records of key Pacific meteorological phenomena, specifically the long-term temperature trend and local manifestations of ENSO and the Pacific Decadal Oscillation (PDO) (Mantua *et al.*, 1997). The study site was thus chosen in Guam's Apra Harbor at Gabgab Beach (Figure 1b,c), a marine preserve and recreational facility inside U.S. Naval Base Guam, only a 30-minute drive from the University of Guam's Water and Environmental Research Institute of the Western Pacific. A 50-year Sr/Ca record from a *Porites lutea* colony was compared with local and regional instrumental records and to the ENSO and PDO indices. The coral Sr/Ca record from this study is the first published for Guam.

To minimize the prospect that environmental variables might perturb results, pristine open-water sites are typically favored for coral paleoclimate proxy studies. The remoteness of such sites, however, limits the number of sites that can be studied over time and precludes intensive study of *in situ* environmental conditions that might affect standard techniques of paleoclimate reconstruction. The principal focus of this study was thus to explore whether coral in an accessible location, although with nonpristine geochemical conditions, might produce adequate records of fundamental Pacific climate phenomena. Monitoring and documenting environmental variables at the site that might affect the record was thus a central component of the study.

The second focus of the study was the utility of the Sr/Ca proxy record not merely for reconstructing sea surface temperature (SST) (for which there is no official local long-term record), but also its relationship to local weather office air temperature records and the ENSO and PDO indices, which reflect other coastal environmental factors that might influence—or even determine—the coral proxy record. The Sr/Ca time series obtained from the coral is therefore meticulously compared with local instrumental records, to the ENSO and PDO indices, and to a regional SST time series. The quality of the historical instrumental records used for comparison is also critically examined.

Although standard field sampling and laboratory geochemical techniques were employed, this study was not a conventional coral paleothermometry study, which would have accordingly been conducted where conditions would be optimal for paleothermometric calibration and verification. The study site was rather at a conveniently located beach, near shore, in shallow water, within an enclosed harbor receiving discharge from inland streams and hosting commercial and naval ports (Figure 1c). Had the principal objective been to maximize the accuracy and precision of the Sr/Ca-SST transfer function, a site would have been selected on one of Guam's pristine reefs on a remote coastal section of its northern limestone plateau, where there is no riverine discharge and large coral colonies thrive in clear, open water at several meters depth, such as Asami *et al.* (2004, 2005) sampled for their previous coral paleoclimate study on Guam.

Related Previous Studies

Asami *et al.* (2005) demonstrated the utility of oxygen and carbon isotope records from a *Porites lobata* core extracted at a pristine open-water site, Double Reef, on NW Guam (Figure 1b). The core yielded a 213-year time series, the final 20 years of which they verified against the instrumental record (Asami *et al.*, 2004). Their results indicated decadal SST variability with 15- to 45-year periodicity of alternating periods of warm-wet *vs.* cool-dry. Shinjo *et al.* (2013) derived a pH proxy record for 1940–1949 from boron isotope composition in a massive *Porites* sp. coral on Guam's NW coast. During the past two decades, numerous Indo-Pacific studies of Sr/Ca records from *Porites* spp. have documented ENSO signals (Calvo *et al.*, 2006; Evangelista *et al.*, 2007; Mitsuguchi *et al.*, 2008; Osborne *et al.*, 2014; Ourbak *et al.*, 2006) and PDO signals (Crueger, Zinke, and Pfeiffer, 2009; Deng *et al.*, 2013; Dima *et al.*, 2005; Evans *et al.*, 2001; Felis *et al.*, 2010; Linsley, Wellington, and Schrag, 2000; Linsley *et al.*, 2015; Liu *et al.*, 2008; Nurhati, Cobb and Di Lorenzo, 2011; Pfeiffer *et al.*, 2009; Rodriguez-Ramirez *et al.*, 2014).

A growing body of literature addresses factors that might affect the Sr/Ca proxy (*cf.* Bell *et al.*, 2017, 2018; Correge, 2006;

DeLong *et al*., 2011; de Villiers, Shen and Nelson, 1994; Flannery and Poore, 2013; Moreau *et al*., 2015; Saenger *et al*., 2008; Smith *et al*., 1979, 2006; Swart, Elderfield, and Greaves, 2002). Recently on Guam, McCutcheon *et al*. (2015) examined the relationship between Sr/Ca-SST results and coral growth rates using coral samples from three sites distributed along a 20-km stretch of Guam's west coast (Prouty *et al*., 2014). Discrepancies between these samples provide further evidence that the reliability of the Sr/Ca proxy may be sensitive to local environmental conditions. To the authors' knowledge, there have been only two studies (Shen *et al*., 1996; Swart, Elderfield, and Greaves, 2002) that obtained *in situ* time-series measurements of seawater Sr/Ca around corals sampled for Sr/Ca SST proxy.

Regional Climate Characteristics

Because this study sought to compare the coral proxy record with local climate more broadly than merely with SST, the essential aspects of Guam's regional climate are summarized below, with emphases on the features against which accuracy and precision of climate proxy measurements should be evaluated and on variables which, besides SST, might influence or correlate with the coral Sr/Ca record—and which might even be amplified in an enclosed-harbor, shallow-water setting such as was selected for this study. It should be noted that given Guam's location in the deep tropics, the monthly averages of SST and the maximum and minimum air temperatures have only relatively small daily and annual ranges. Other variables have large variation, particularly monthly rainfall, which has about a 1-m difference between the respective 6-month sums of the dry and wet seasons.

Seasonal Variability

Guam is located on the eastern edge of the western Pacific monsoon system (Wang and Ho, 2002), with episodic incursions of southwesterly wind flow throughout the summer and fall replaced by persistent trade winds through the winter and spring. The weather of summer through fall is governed by the monsoon trough, near which are heavier rain showers, thunderstorms, monsoon squalls, and an increased risk of typhoons. All the weather elements on Guam vary with the seasonal advance and retreat of the monsoon trough and the months-long dry-season immersion in the Pacific trade wind system.

Guam has distinct dry and rainy seasons, with 30% of its annual rainfall occurring January through June, and 70% during July through December. The rainfall total during the three wettest months (centered on September) is about 1000 mm (39 inches). During the three driest months (centered on March) the total is only 300 mm (12 inches). Large interannual variations also occur, with the observed annual total varying by a factor of three (*i.e*. from 1250 to 3750 mm [50 to 150 inches]). Air temperature and sea surface temperature have relatively small seasonal variation (by midlatitude standards). The mean maximum temperature of the warmest month—for example, at the Andersen Air Force Base (AAFB) observing site (station elevation = 160 m)—is 1.7°C warmer than the coldest month (29.5°C *vs*. 27.8°C, respectively). The SST around Guam has a similar seasonal range as Guam's air temperature, with a spread of 2.0°C between the 27.4°C average SST of the coolest month (February) to the 29.4°C average of the warmest month (September). This 2.0°C average range of the annual cycle of SST and the 0.084 mmol/mol average range of the annual cycle of Sr/Ca are thus used as comparative benchmarks with which to assign temperature values to variations of Sr/Ca. The obvious banding observed in the coral sample is thus assumed to be sensitive to this small 2.0°C change of SST, but it is noted that it could also, or otherwise, be responding to other seasonal variables that also exhibit regular and persistent annual cycles, such as the amount of daily sunshine and the timing and magnitude of the extreme lower low tides.

Interannual and Interdecadal Natural Variability

Guam and all of Micronesia are located in an ENSO core region (Ropelewski and Halpert, 1987), with a consistent evolution of local climate variables associated with each phase of ENSO, particularly during the occurrence of El Niño. All the climate variables—including SST, sea level, air temperature, rainfall, and typhoon distribution—are thus likely to exhibit (and perhaps, track) the large interannual fluctuations that are present in any time series of an ENSO index. Indeed, the ENSO cycle is the dominant driver of Guam's interannual climate variation. The average period of ENSO is 3.6 years, with a range of 2–7 years (Dean and Kemp, 2004). The variability associated with the canonical ENSO and the newly described ENSO Modoki (Ashok *et al*., 2007) explain 57% of the variance of Pacific SST (Messie and Chavez, 2011).

At even longer timescales than ENSO, another important large-magnitude, basin-wide cycle of Pacific SST and other climate variables is the PDO (Francis and Hare, 1994). The spatial patterns of the PDO resemble those of the ENSO cycle in lower latitudes but have a larger amplitude than ENSO in midlatitude and high latitude. As with the ENSO cycle, the PDO has warm/positive and cold/negative phases that may persist for 20–30 years (far longer than the phase shifts of ENSO). It has been hypothesized that the PDO modifies the character of the ENSO cycle itself (Newman, Compo, and Alexander, 2003; Wang *et al*., 2014). Capturing ENSO and PDO signals are thus desired goals—and crucial tests—of west Pacific climate reconstruction.

The daily tide on Guam exhibits a mixed semidiurnal signal, with two roughly equal high tides and two often very different low tides. The mean annual difference between the daily high and low tides is 0.8 m (2.6 feet). The large historical interannual and interdecadal variation of Guam's regional sea level has been shown to be predominantly an artifact of regional trade wind forcing (Merrifield, Thompson, and Lander, 2012). The variations of Pacific trade winds, however, are themselves linked to ENSO, especially at low latitudes across the Pacific, where during El Niño the trade winds weaken, and during La Niña the trade winds strengthen. The range of variability of sea level at ENSO timescales (0.6 m) is nearly identical to the daily range of the astronomical tide.

Local Historical Climate Records

Because of its militarily strategic location in the western Pacific, Guam, along with other U.S.-affiliated Pacific islands in the region, is endowed with robust instrumental infrastructure and reliable climate records going back to at least the end of World War II. There is at least one first-order weather station at each of the major island groups of Micronesia with a

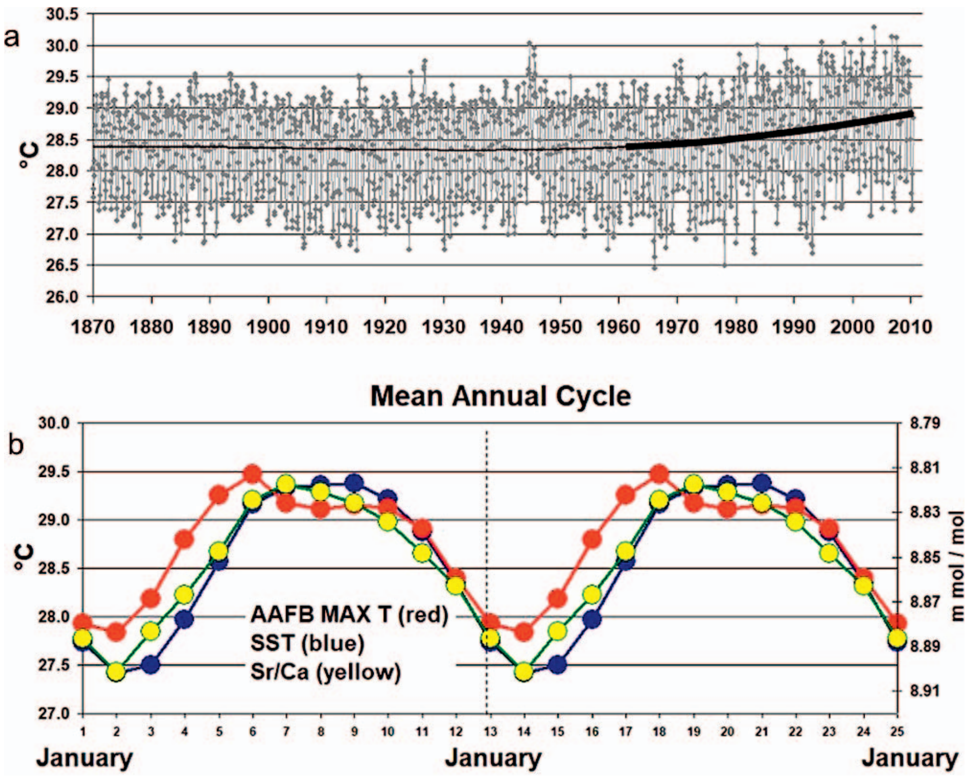

Figure 2. (a) Time series of SST in the Hadley 1°×1° grid cell encompassing Guam (SW anchor point at 13° N, 144° E). Values plotted are monthly averages. Black line is the best fit third-order polynomial. The thick part of the black line is the portion of the SST trend line overlapping the period (1960–2010) of the Gabgab Sr/Ca time series. (b) The mean annual cycle for AAFB maximum temperature (red), Hadley SST (blue), and coral Sr/Ca (yellow). Each maximum of the coral Sr/Ca was assigned to February, with all other values of Sr/Ca interpolated within February-to-February bins. By pinning the maximum value at February, the mean annual cycle of the Sr/Ca exhibits a nonsinusoidal asymmetry, such that the timing of the February minimum to the July maximum is 5 mo, whereas the timing of the July maximum to the next February minimum is 7 mo. The annual cycles of both the air temperature and the SST also possess nonsinusoidal asymmetries: The air temperature peaks in June (only 4 mo after its February minimum), and the SST peaks in September (a full 7 mo after its February minimum). Please note that the scale for the Sr/Ca is inverted to facilitate visual comparison.

nearly complete record of rainfall and air temperature from post–World War II to present. Guam has only one station, AAFB, with a continuous climate record of daily maximum-minimum temperature and daily rainfall and with instrumentation that has remained at the same location and in the custody of the same organization. The AAFB airfield climate record (containing daily maximum and minimum temperature and daily rainfall) on file at the National Climate Data Center (NCDC) has many missing days (2.5%) and several missing months (15) over the listed period of record (1953–2002) and has not been updated at NCDC since 2002. The complete record is available locally and is used in this study.

The sea level on Guam has been measured continually and accurately from 1948 to present and is available on the website of the University of Hawaii Sea Level Center. Other climatic variables such as SST, percent daily sunshine, daily mean wind speed and direction, barometric pressure traces, *etc*. have not been extensively measured or archived for Guam. Some measurements, such as SST, are available online as a blend of *in situ* recordings with satellite data. The local SST time series used for this study (Figure 2a) was extracted from the nearest grid cell in the Hadley global SST data set. The Hadley SST data set (HadISST1, through 2010) was chosen because of its wide use and its use by Asami *et al*. (2005). The annual cycle of SST (Figure 2b) is of great importance for this study because the annual cycle exhibited by the coral Sr/Ca time series was pinned to it.

Harbor Environmental Conditions

There has yet to be a detailed study of the water budget or circulation within Apra Harbor, but some observations of local geologic and hydrologic conditions provide useful initial assessments of the potential for dilution and sediment input by freshwater, from either direct rainfall into the harbor, coastal seepage, or surface-stream runoff from the adjacent watershed (Figure 1c). Such events and conditions, of course, can be expected to correlate with rainfall and other weather variables. Some initial insight into the prospects for rainfall-related changes in harbor conditions is gained by comparing the mean daily freshwater input to the harbor from the wettest month on record, August 2004, with the mean daily input for the period of record (1961–2005). (August is on average the wettest month on Guam.) For the period of record (based on Johnson, 2012; A.G. Johnson, unpublished data), the mean

Table 1. *Apra Harbor hydrologic statistics.*

Area of inland watershed		Harbor area	Harbor volume	Harbor mean depth
acres	m^2	m^2	m^3	m
8064.5	3.26E+07	1.54E+07	3.20E+08	20.78

Mean monthly totals and maximum for August 1961-2005	Monthly rainfall and evapotranspiration (Johnson, 2012)				Mean daily volume input per unit area (m/m^2)			
					Watershed	Harbor	Total freshwater input	
	Rainfall (P) inches	Evapo-transpiration (ET) inches	P-ET		Runoff into harbor	Direct input to harbor	runoff + direct input	
			inches	meters			meters	% harbor depth
August mean	14.86	4.93	9.93	0.252	0.017	0.012	0.029	0.14%
August 2004	38.00	4.93	33.07	0.840	0.057	0.031	0.089	0.43%

Extreme daily events	Daily rainfall and evapotranspiration (NOAA)				Mean daily volume input per unit area (m/m^2)			
					Watershed	Harbor	Total freshwater input	
	Rainfall (P) inches	Evapo-transpiration (ET) inches	P-ET		Runoff into harbor	Direct input to harbor	runoff + direct input	
			inches	meters			meters	% harbor depth
Typhoon Pamela, 24 May 1976	31.00	0.16	30.84	0.783	1.660	0.787	2.448	11.78%
Continuous thunderstorm 26 Feb 1980	8.24	0.16	8.08	0.205	0.435	0.209	0.644	3.10%

daily direct rainfall into the harbor was 12 mm, plus an equivalent of 17 mm as coastal seepage and runoff from the adjacent watershed, for a total of 29 mm, which is 0.14% of the mean harbor depth of 21 m (Table 1). For August 2004, the sum of the mean daily inputs—direct input and runoff equivalent—is three times the long-term mean, or 0.43% of mean harbor depth. For the heaviest daily rainfall on record, from Typhoon Pamela on 24 May 1976, the total freshwater input to the harbor constituted about 12% of the mean harbor depth.

There have been no studies of harbor sedimentation dynamics, but the sample site appears to be protected from stream-borne sedimentation. The streams that enter the harbor discharge onto alluvial aprons that support dense coastal wetland vegetation enclosed behind the inner harbor. The inner harbor is fronted by shallow coral reefs at the back of the outer harbor (Figure 1c). The mouth of the harbor spans ~0.5 km, from which the channel bottom rises from ~150 m to generally ~120 m depth along the central axis of the harbor. Given the study site's location in the outer harbor, ~4.5 km from the inland side and 2.8 km from the harbor mouth, where it stands on the flank of the harbor's deep water, it is thus likely protected from all but the most extreme sedimentation events and probably has a rapid flushing rate.[2] Inside this physically sheltered area, the reef is generally healthy, supporting abundant and diverse fauna.

The limestone terrain of the peninsula on which the beach is located supports no streams or visible permanent springs, and the small size of the catchment behind the beach implies that seepage flux next to the study site is modest and short-lived. Local overland flows from heavy storms are rare and short-lived. Nevertheless, to ascertain seawater composition around the site and how it might be affected by such conditions as described above, this study included a 16-month program of systematic environmental sampling of the seawater at the site.

METHODS

This section describes the instrumentation and sampling regimen applied at the study site to assess local environmental conditions, and the extraction and laboratory analysis of the coral sample.

Environmental Monitoring at the Site

Data collection began September 2009 at a *P. lutea* colony 120 m offshore near the margin of the reef at Gabgab Beach (Figure 3). Environmental data were collected at the site beginning September 2009 (10 months before extracting the coral core sample in July 2010) through September 2010 (2 months after collection of the core). Environmental monitoring included regular collection of seawater samples for δ^{18}O, pH, cations (Mg, Ca, K, Sr, B, Ba), and nitrate and continuous logging of water temperature and salinity at the base of the coral (Figures 4–7). Monthly seawater samples were collected by diving to the base of the coral head and filling a 4-mL glass vial for δ^{18}O analysis (Figure 4a); a 30-

[2]On 26 February 1980, one of the authors of this paper (Lander) witnessed the effect on the harbor from a heavy rainfall event wrought by a local continuous thunderstorm event (*cf*. Ramage, 1995). This 10-inch (25-cm) event put about one-quarter of the Typhoon-Pamela volume into the harbor. The water in the entire harbor, as seen from the shore, was colored bright red from the sediment carried in by the streams from the adjacent watershed (Figure 1c). The appearance of the harbor returned to normal within a few days. It has thus been observed, even though not formally documented, that occasional extreme events can introduce substantial sediment pulses into the harbor.

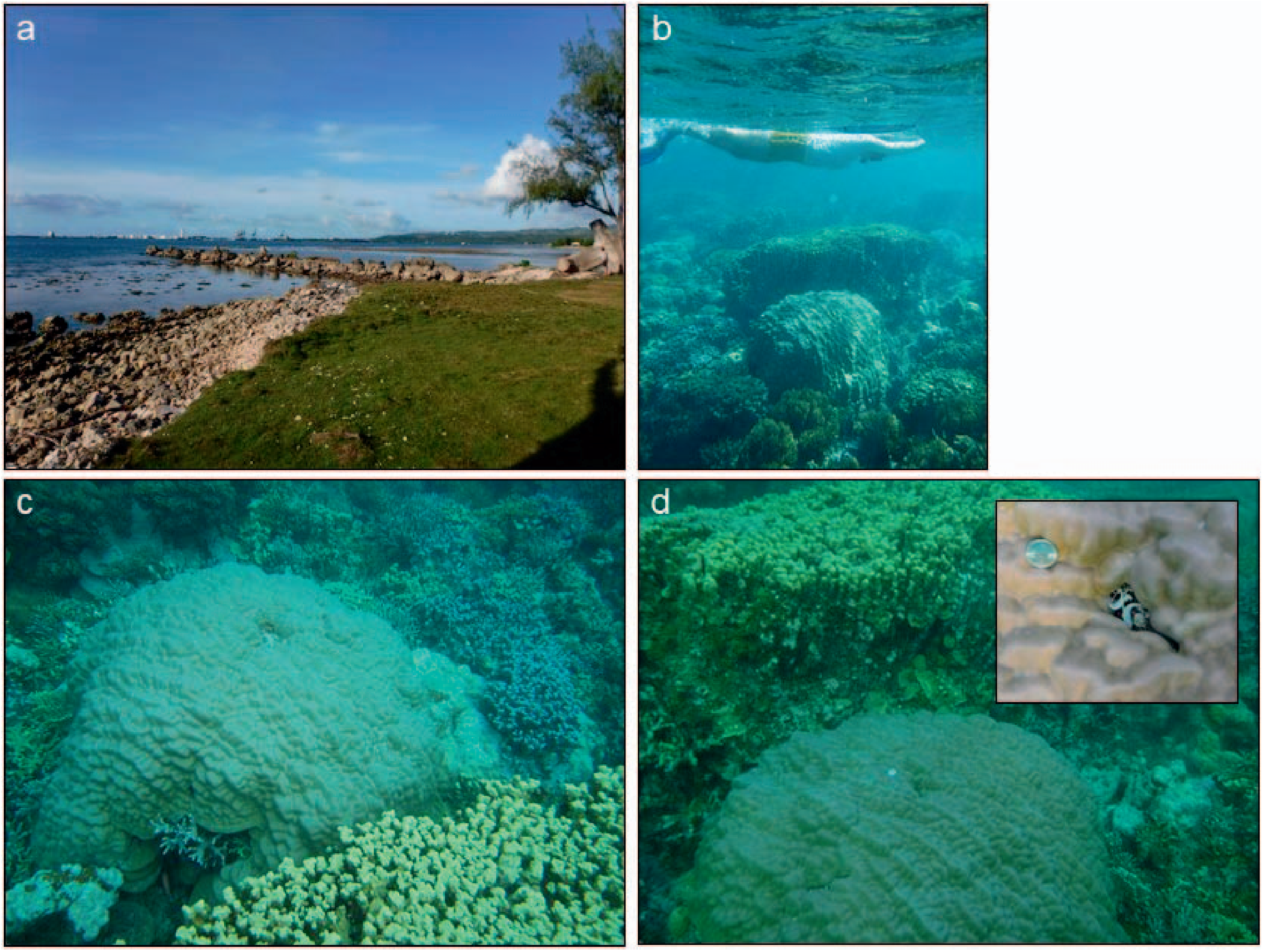

Figure 3. (a) Gabgab Beach sampling site, looking NE toward the civilian port facilities. The location of the sampled coral lies 37 m directly off the end of the 90-m-long artificial jetty. The Apra Watershed is in the background on the right-hand side. Photograph taken at extreme low tide (~0.5 foot below mean low-low) 17 June 2018. (b) Sampled coral (*Porites lutea*, bottom foreground) lies at about 2 m depth, as measured on the day of the photograph. The coral head is 1.0 m in diameter (circumference 3.5 m) and stands 0.5 m above its base, which is at 2.5 m depth. The top of the coral head is thus at about 2 m depth. Photograph taken 21 October 2016. (c) Coral head 12 May 2012, nearly 2 y after core extraction (26 July 2010). Maximum diameter of the scar in the top center of the colony is 8 cm, the diameter of the core. (d) Coral head 7 April 2018, nearly 8 y after core extraction. Scar is visible at the top center of the coral. U.S. quarter-dollar next to it at the ten o'clock position. (d inset) Close-up of drilling scar taken 17 June 2018. U.S. quarter-dollar for scale.

mL polyethylene bottle for cation analyses; a 50-mL vial for filling the sensor wells of a Myron Ultrameter II, by which to measure pH (Figure 4b); and a 50-mL polyethylene bottle for nitrate (Figure 4c). Seawater δ^{18}O from the site was analyzed at the University of Texas-Austin by isotope ratio mass spectrometry, with an analytical precision of 0.1‰ (2σ). For nitrate analyses, samples were transported within an hour to the Water and Environmental Research Institute of the Western Pacific (WERI) Water Chemistry Laboratory at the University of Guam, where they were frozen, and then analyzed for nitrate within 30 days of the sampling date by flow injection analysis, with a detection limit of 0.0008 mg/L and analytical precision of $\pm$0.005. Samples for cations (Table 2 and Figure 5) were acidified with 2% trace metal–grade nitric acid and analyzed at the U.S. Geological Survey facility at Menlo Park, California, by inductively coupled plasma mass spectrometry. The precision was determined by analyzing a series of multi-elemental standards made from commercially available single-element stock standard solutions run at intervals during the session. The relative standard deviation for each species was Sr, 1.53%; Ca, 1.36%; Mg, 2.12%; K, 1.95%; B, 3.26%; and Ba, 1.28% (Table 2). Gaps in the time series reflect typical challenges of field sampling programs, including bad weather, no-notice beach closures, and pilfering of instruments by beach-goers.

In situ temperature data (Figure 6) were obtained at 60-minute intervals from Onset Tidbit loggers (v2 UTBI-001) installed at the base of the Gabgab coral before sampling from

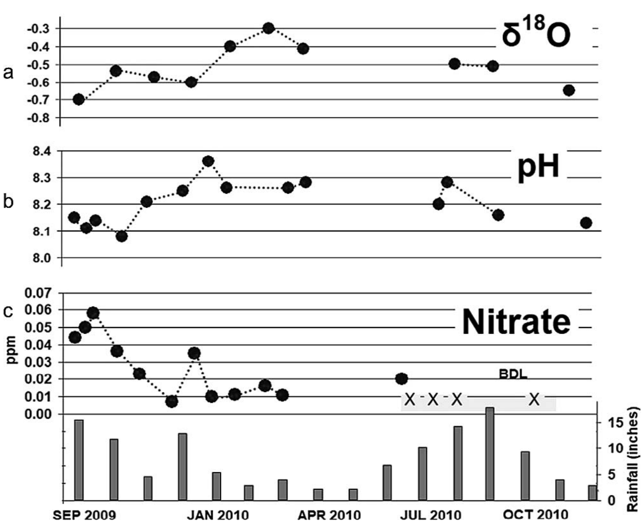

Figure 4. (a) Seawater $\delta^{18}O$ at the Gabgab site *vs*. monthly rainfall from the nearby USGS Mount Chachao rain gauge (bars at the bottom). In spite of gaps, the seawater $\delta^{18}O$ data suggest a negative correlation with the annual cycle of rainfall. (b) Seawater pH at the Gabgab site *vs*. monthly rainfall. The seawater pH data suggest a negative correlation with the annual cycle of rain. (c) Seawater nitrate concentration (ppm) at the Gabgab site *vs*. monthly rainfall. Low measurements beginning in July 2010 were below detection limits (shown with and x in the gray bar). There is no apparent systematic relationship between nearby rainfall and nitrate concentration at the site.

September to December 2009; again, during the month of July 2010 (near the end of which the core sample was drilled); and

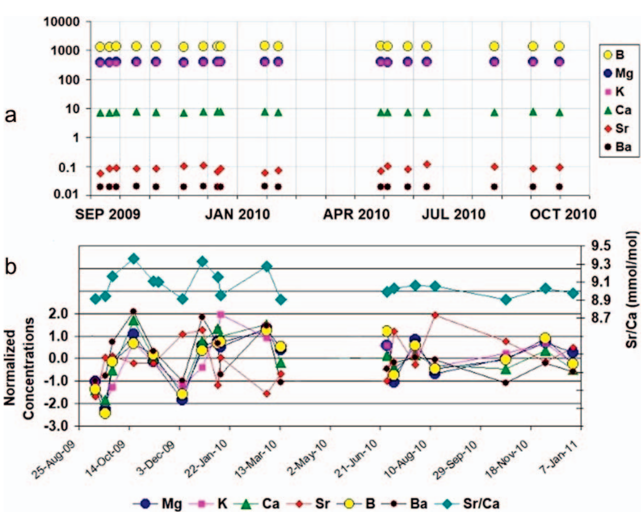

Figure 5. (a) Time series of concentrations (ppm) for the major seawater cations at the Gabgab site. (b) Variability about mean concentration for each species, normalized to its standard deviation. Standard deviation as a percentage of the mean was 2%–3% for each species except Ba, for which it was about 20%. The Sr/Ca ratio has been included in the bottom panel. Note: the bottom panel (b) contains the same information as in the top panel (a), but the scale has been exaggerated to reveal the variability. When this is done, the coherence of the variation among the cations is also revealed. The variability of Sr seems to be the most out of step with the pack.

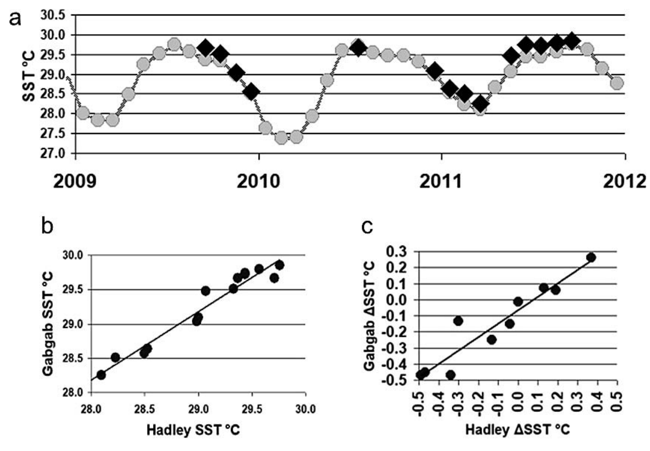

Figure 6. (a) Measured Gabgab SST (black diamonds) compared with the Hadley SST (open circles). (b) Scatterplot of the raw data. (c) Scatterplot with the serial correlation removed as ($GSST_{(t+1)} - GSST_{(t)}$) *vs*. ($HSST_{(t+1)} - HSST_{(t)}$).

again from December 2010 through September 2011. Data gaps reflect instrument failure and pilfering. One month of continuous high-resolution salinity and temperature data (Figure 7) were obtained during July 2010 from a JFE Advantech Infinity CT logger, also installed at the base of the coral. Further attempts at continuous logging of conductivity/salinity were discontinued after the instrument was taken by a self-described environmental activist who claimed the instrument was harming the reef.

Extraction and Laboratory Analysis of the Coral Core

On 26 July 2010, a coral core 80 mm in diameter and 94 cm long (Figure 8a) was extracted vertically from near the center of a *P. lutea* colony (Figure 3b–d) at a water depth of 1.9 m and standing 120 m seaward from Gabgab Beach (Bell *et al*., 2011, 2012). In the laboratory at the University of Texas-Austin, a 12-mm-thick slab was cut along the axis of the core. The slab was washed in an ultrasonic cleaner for 60 minutes on each side and then oven-dried overnight. Samples were drilled at 1.2-mm intervals to obtain approximately monthly resolution. A total of 733 samples, each 1.2-mm wide by 0.5-mm deep, was extracted by a computer-controlled Micro-Mill®. Each sample was weighed, digested with 2% nitric acid, and analyzed for Sr/Ca by inductively coupled plasma optical emission spectroscopy with a precision of 0.013 mmol/mol.

X-ray radiography images were taken to identify annual growth bands discerned from high- and low-density couplets (Figure 8a). Skeletal features in the core are well preserved and well expressed, with no visible signs of diagenesis seen in visual inspection of the slab or the x-ray image. The average thickness of the coral bands was about 1.5 cm and fairly uniform (1.44 ± 0.12 cm (1σ) (Figure 8b). More intensive inspection for diagenetic alteration by x-ray diffraction or electron microscopy was thus deemed unnecessary.

The raw geochemical data (Figure 9) were linearly interpolated to 12 points per year, yielding an effective monthly resolution by the AnalySeries (v. 2.0.4) application (Paillard,

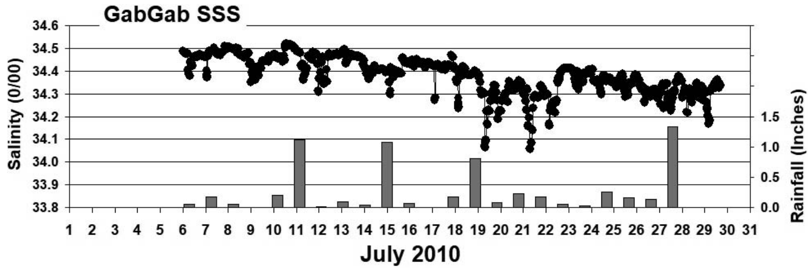

Figure 7. Hourly salinity (parts per thousand) measured at the Gabgab site *vs*. daily rainfall (inches) for July 2010. Daily rainfall was obtained from a USGS rain gauge at the nearby Mount Chachao site. July 2010 was drier than average on Guam, but the salinity shows, in general, a gradual decline of about 0.2 mil over the course of the month, which is consistent with the onset of the wet-season rainfall.

Labeyrie, and Yiou, 1996). On the basis of instrumental and *in situ* data, the lowest SST occurs in February; therefore, the highest Sr/Ca value in each annual band was assigned to February. With the Sr/Ca time-series maxima pinned to February, the Sr/Ca minima consistently fall between the June air temperature peak and the September SST peak. Coral band thicknesses spanned as few as nine to as many as 14 raw data points. Because the average value of the number of raw data points between anchor points was 12, the interpolated time series does not vary much from the raw data sequence. At some places on Figure 9, one may, on close examination, see that the effect of interpolation was to reduce the magnitude of some of the spikes in the raw data and to shift the maxima and minima a month or two left or right.

RESULTS

This section describes seawater characteristics at the study site, the Sr/Ca time series obtained from the core sample, and comparison of the Sr/Ca time series with regional SST, local air temperature, and large-scale Pacific climatic signals, specifically ENSO and the PDO.

In situ Seawater $\delta^{18}O$, pH, Cations, Temperature, Salinity, Nitrate

Seawater $\delta^{18}O$ at the site ranged from –0.70‰ in September 2009 to –0.30‰ in February 2010, with the isotopic ratios

Table 2. *Gabgab seawater analytical results.*

Sample Collection Date	Gabgab Cation Concentrations (ppm)						Cation/Ca Ratios				
							mol/mol			mmol/mol	
	B	Mg	K	Ca	Sr	Ba	B/Ca	Mg/Ca	K/Ca	Sr/Ca	Ba/Ca
10 Sep 09	5.23	1323.87	390.11	374.14	7.29	0.059	0.052	5.83	1.07	8.91	0.046
20 Sep 09	5.36	1294.22	378.74	367.81	7.19	0.087	0.054	5.80	1.06	8.94	0.069
27 Sep 09	5.32	1357.73	399.01	373.15	7.48	0.088	0.053	6.00	1.10	9.16	0.069
18 Oct 09	5.60	1380.98	410.28	388.48	7.95	0.083	0.053	5.86	1.08	9.36	0.062
7 Nov 09	5.49	1367.22	398.55	381.63	7.60	0.083	0.053	5.91	1.07	9.10	0.063
6 Dec 09	5.39	1317.94	382.34	373.68	7.28	0.104	0.053	5.82	1.05	8.91	0.081
26 Dec 09	5.50	1372.27	405.38	380.08	7.75	0.107	0.054	5.95	1.09	9.32	0.082
10 Jan 10	5.70	1381.18	407.28	393.08	7.87	0.067	0.054	5.79	1.06	9.16	0.050
13 Jan 10	5.69	1382.80	404.74	398.15	7.79	0.087	0.053	5.73	1.04	8.95	0.064
28 Feb 10	5.60	1396.68	412.88	390.28	7.91	0.061	0.053	5.90	1.08	9.27	0.046
14 Mar 10	5.69	1376.42	403.78	387.98	7.55	0.075	0.054	5.85	1.07	8.90	0.056
28 Jun 10	5.58	1395.47	405.47	387.57	7.62	0.070	0.053	5.94	1.07	8.99	0.053
5 Jul 10	5.55	1341.27	389.96	379.82	7.50	0.106	0.054	5.82	1.05	9.03	0.081
26 Jul 10	5.50	1377.89	407.88	384.75	7.62	0.082	0.053	5.91	1.09	9.06	0.062
15 Aug 10	5.32	1349.23	393.64	380.19	7.52	0.118	0.052	5.85	1.06	9.05	0.090
24 Oct 10	5.43	1360.75	400.14	384.88	7.49	0.099	0.052	5.83	1.07	8.90	0.075
3 Dec 10	5.37	1387.18	406.55	388.15	7.66	0.084	0.051	5.89	1.07	9.03	0.063
30 Dec 10	5.44	1355.21	402.58	381.50	7.48	0.094	0.053	5.86	1.08	8.97	0.072
Maximum	5.70	1396.68	412.88	398.15	7.95	0.118	0.054	6.00	1.10	9.36	0.090
Mean	5.49	1362.13	399.96	383.07	7.59	0.086	0.053	5.86	1.07	9.06	0.066
Minimum	5.23	1294.22	378.74	367.81	7.19	0.059	0.051	5.73	1.04	8.90	0.046
SD†	0.14	27.24	9.24	7.52	0.21	0.016	0.001	0.06	0.01	0.14	0.013
RSD%†	2.48	2.00	2.31	1.96	2.73	18.40	1.54	1.08	1.38	1.56	19.12
Lab SD†	1.08	0.03	0.01	0.07	0.85	0.15					
Lab RSD%†	3.26	2.12	1.95	1.36	1.53	1.28					

†*Standard deviations (SD) and relative standard deviation percentages (RSD%) are based on a series of multielemental standards built from commercially available single-element stock standard solutions. The precision is determined by reproducibility of a lab quality-control sample (Lab) run at intervals during the session.*

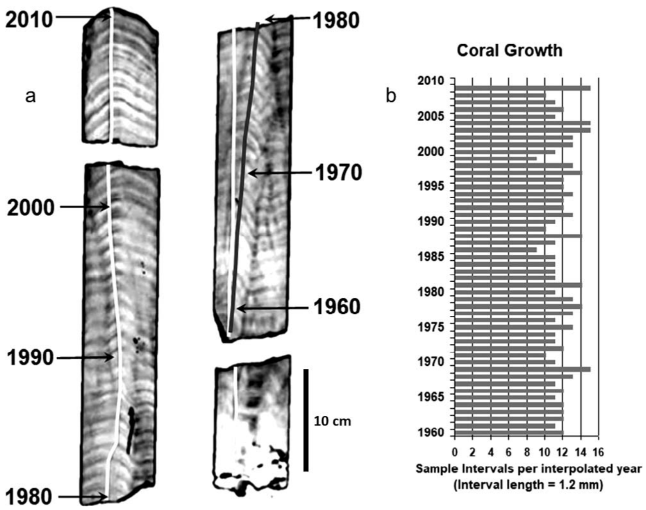

Figure 8. (a) X-ray (positive image) of the core from the *Porites lutea* colony shown in Figure 3. Arrows show the intersection of the sampling track, with the lightest color band marking each annual interval. (The track followed from 1979 to 1960 does not appear on the x-ray because it was a second track, made after the x-ray was taken, to follow the growth axis more closely than the initial track, which is the one that appears on the x-ray.) (b) Approximate annual growth based on sampling interval counts per interpolated year.

showing an inverse relationship to monthly rainfall through the study period (Figure 4a). This is consistent with the amount effect (Craig, 1961) seen in rainwater (*i.e*. the greater the amount of rainfall, the lower the $\delta^{18}O$). Guam rainwater isotope data reported by Partin *et al*. (2012, figure 7) showed peak wet season rainwater to be strongly depleted in ^{18}O (on the order of –8‰). The pattern seen in the seawater samples from the Gabgab site thus most likely reflects the input (from

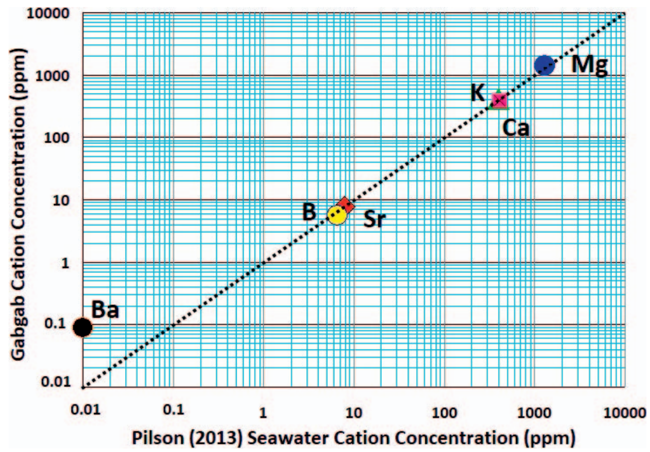

Figure 10. Mean concentrations (ppm) for each cation time series at the Gabgab site (vertical axis) compared with Pilson's (2013) mean global values for seawater (horizontal axis). The only departure from uniformity is Ba, for which the mean concentration at the Gabgab site is about an order of magnitude higher than the mean global value.

both direct rainfall and river water) of ^{16}O-enriched (^{18}O-depleted) rainwater during the rainy season. Monthly on-site measurements of pH (Figure 4b) ranged from ~8.1 in the wettest months to ~8.3 in the dry months. The slightly lower pH in the wetter months also seems consistent with freshwater input from precipitation, which has lower pH than the seawater.

Monthly nitrate concentrations at the site (Figure 4c) dropped more or less steadily from a high of 0.6 mg/L at the start of sampling in September 2009 to below the detectable limit (<0.1 mg/L) by July 2010 and thence remained below detection limits through the end of the sampling period in

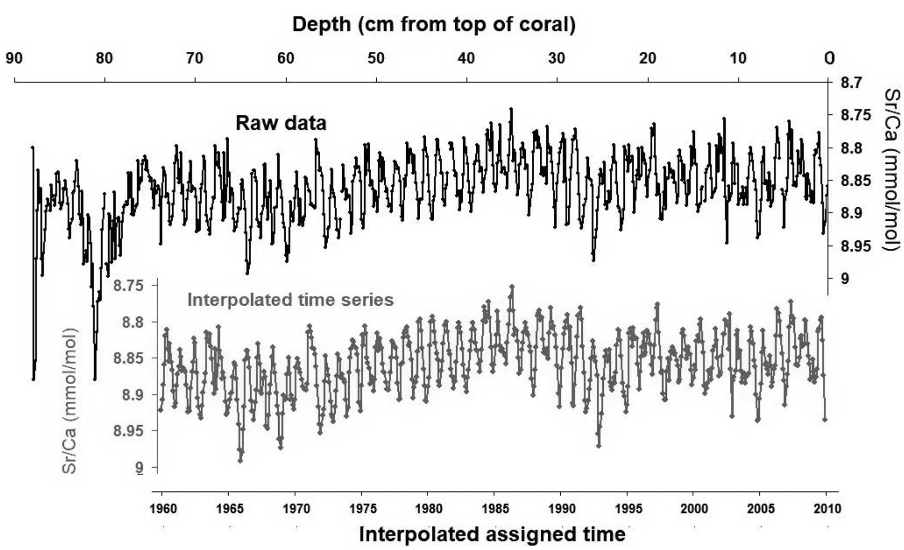

Figure 9. Gabgab coral raw data in two frameworks: (1) with respect to distance from the top of the coral (top) and (2) interpolated by fixing each annual maximum to the month of February (bottom). (Please note inverted scale for Sr/Ca).

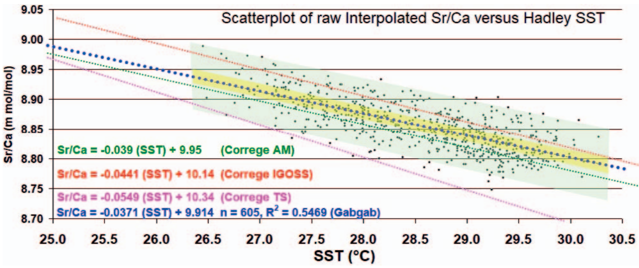

Figure 11. Scatterplot of Gabgab interpolated Sr/Ca *vs*. Hadley SST (604 points spanning 1960–2010). Blue dotted line is best fit linear trend (blue equation at bottom left). Other lines are transfer functions computed by Correge (2006) for a *Porites lutea* coral in the SW Pacific. "AM," "IGOSS," and "TS" are different SST records used by Correge to derive his transfer functions. Light green shading shows the 95% prediction interval, and light yellow shading shows the 95% confidence interval of the blue regression line.

December 2010. Marubini and Davies (1996) reported results of an experiment using *Porites porites* and *Montastraea annularis* that indicated that nitrate concentrations greater than 1 μM/L (0.062 mg/L) reduce skeletogenesis in corals. On the other hand, Atkinson, Carson, and Crow (1995), in a study of 57 species of cultured coral in the Waikiki Aquarium, reported that growth of corals was not inhibited by concentrations of nitrogen up to 0.31 mg/L. By either result, the nitrate concentrations observed at the Gabgab sample site would not likely be high enough to affect coral calcification.

Between September 2009 and December 2010, seawater Sr/Ca ratios ranged from a minimum of 8.90 to a maximum of 9.36 mmol/mol, with an average value of 9.06 mmol/mol (Table 2). Overall, Sr/Ca values from Apra Harbor are enriched by ~0.5 mmol/mol relative to previously reported Sr/Ca values from the Pacific (de Villiers, Shen, and Nelson, 1994; Shen *et al*., 1996). The time series for each cation concentration (Table 2 and Figure 5a) shows it to be essentially uniform and stable over the study period. Standard deviation as a percentage of the mean for each time series was 2%–3% for each species except Ba, for which it was ~20%. A plot of the concentrations normalized to the standard deviations about their respective means (Figure 5b) reveals no apparent systematic variation for any of the species. The fluctuations of concentration for all species appear, however, to be generally correlated (*i.e*. rising and falling together), with the curious exception of Sr. For each species, the series means plotted against representative global seawater values (as compiled by Pilson, 2013, table 4.1) show close matches (Figure 10), with the single exception of Ba, for which the concentration at the site is about an order of magnitude higher than the Pilson (2013) value. The larger value for Ba can be interpreted as reflecting the presence of river-borne, terrigenous, fine-grained sediment (*cf*. Montaggioni *et al*., 2006; Prouty *et al*., 2014).

Seawater temperatures measured at the Gabgab site (Figure 6) during the study period closely matched the regional Hadley SST record. The salinity time series for July 2010 (Figure 7) exhibited a very small standard deviation of 0.08‰ ($n = 5690$). Comparison of the salinity data to the daily rainfall did not show strong correlation ($r = -0.20$). Seawater salinity at the Gabgab site exhibited a slight general decrease of about 0.2‰, from ~34.45‰ to ~34.25‰. There is no ready explanation for the off-trend drop and recovery in salinity from 18 to 22 July. The overall downward trend, however, may reflect ongoing dilution (by which, whatever evaporation occurred was overcome by direct and riverine inputs) from the onset of the 2010 wet season in June and July. The year 2010 was extraordinarily dry, about 30% below normal, with total annual rainfall at AAFB at only 1836 mm (72.28 inches) compared with the long-term average of 2540 mm (100 inches). In the 5 months leading up to June 2010, AAFB recorded only 460 mm (18.12 inches) of rain. June and July saw 228 and 217 mm (8.96 and 8.56 inches) of rain, respectively, for which the total, 445 mm (17.52 inches), is 97% of the volume recorded in the preceding 5 months. Continuous salinity logging had to be terminated at the end of July because of tampering and the potential for pilfering of the logger, which was too large to hide.

Sr/Ca Time Series from the Gabgab Coral Sample

As a first step toward aligning the Sr/Ca values with the modern climate record, the raw Sr/Ca values were plotted with respect to their distance from the top of the coral core (Figure 9). Because of slight variations in the lengths of the annual bands, the plot of Sr/Ca values *vs*. core depth does not linearly track elapsed time. For this reason, the Sr/Ca time series was interpolated (see the "Methods" section). The growth bands near the base of the core (Figure 8) were irregular and yielded anomalously high Sr/Ca ratios, most likely because of the presence of marine aragonite cements. The 126 raw data points (shown for the raw-data curve) from these suspect growth bands were thus discarded. Therefore, the interpolated time series shown in Figure 9 begins at the 50th growth band from the top of the coral core, with raw datapoint number 606 assigned to February 1960 and raw datapoint number 5 assigned to February 2010. The transfer function obtained from a scatterplot of the interpolated values of Sr/Ca *vs*. the Hadley SST (Figure 11) is used to assign the following linear SST scale (the Gabgab transfer function) to the interpolated time series:

$$\text{Sr/Ca} = -0.037 \times \text{SST} + 9.91 \qquad r = -0.74, n = 605 \qquad (1)$$

Because of the nonoptimal setting of Apra Harbor, it was not assumed at the outset that the Sr/Ca-SST transfer function obtained for the Gabgab coral sample would necessarily be consistent with extant local and regional Sr/Ca-SST transfer functions. However, three transfer functions obtained by Correge (2006) from an analysis of a South Pacific (specifically, New Caledonia, a site similar to Guam in that it is located in the WPWP) *porites* coral core are each close to Equation (1). Beyond noting that these results are consistent with one another, no claim is made regarding the relative robustness of the Gabgab transfer function. Obtaining a regional-standard transfer function was not the goal of this effort. Rather, the Gabgab coral sample was obtained to determine if—in spite of its environment—it held any useful signal of the historical climate record, and, indeed, four prominent local climate signals are reproduced. These are discussed next.

Comparisons of Gabgab Proxy Results with Concurrent Meteorological Records

Elements of local climate seen in the analysis of the Gabgab Sr/Ca time series include (1) an annual cycle, (2) a long-term

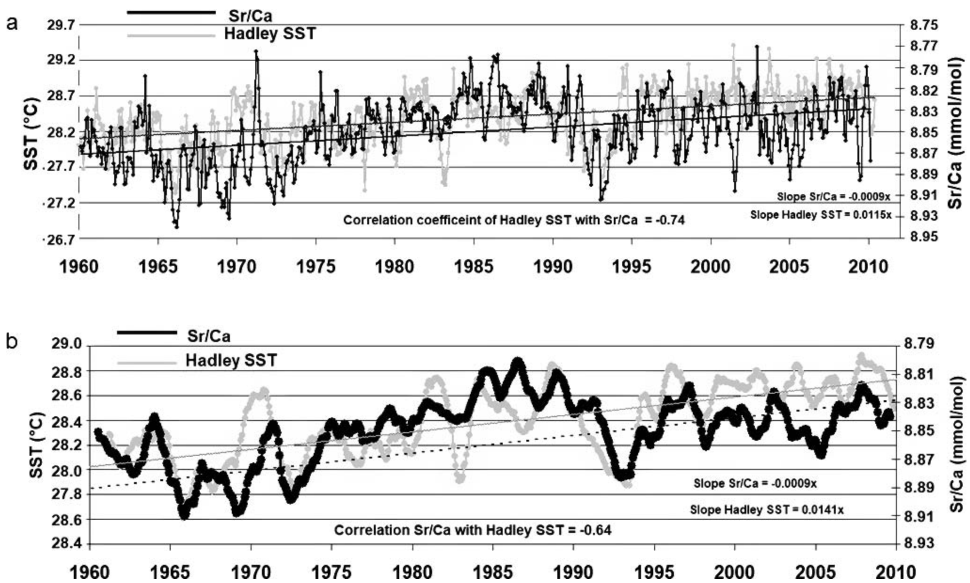

Figure 12. (a) Raw unsmoothed Sr/Ca *vs*. Hadley SST. Black curve is the Gabgab Sr/Ca, and the gray curve is the Hadley SST. Slope of the trend lines for each time series have been included. The correlation coefficient between the two time series of –0.74 is indicated (note inverted scale for Sr/Ca). (b) Raw Sr/Ca *vs*. Hadley SST. Each time series has been smoothed by application of a 12-mo moving average. Black curve is the Gabgab Sr/Ca, and the gray curve is the Hadley SST. The trend lines for each time series have been plotted. The correlation coefficient between the time series of –0.64 is indicated. The annual cycle in each of the time series thus enhanced the strength of the correlation value in panel (a) compared with that in panel (b), in which the annual cycles have been eliminated by the 12-mo smoothing. By removing the linear trends present in each time series (not shown), the cross-correlation between Sr/Ca and SST is reduced further still to –0.47.

trend, (3) interannual variations, and (4) interdecadal variations. The most noteworthy result is the fidelity with which interannual variations in the Sr/Ca time series track the ENSO index and the interdecadal variations track the PDO index.

Annual Cycle of Sr/Ca and SST

Annual cyclicity of the Sr/Ca time series was to some degree forced by assigning sequential maxima to the month of February (see Figure 2b). These assignments, however, were also checked for consistency with the coral banding (see Figure 8a). The raw data were not so noisy as to mask the large periodic sinusoidal variation of the annual cycle, which is obvious even in visual inspection. The June peak of air temperature on Guam is explicable by relatively clear skies and light winds during June followed by an abrupt increase of cloudiness, rainfall, and (sometimes) monsoonal winds during July. The September SST peak shows a typical lag of peak insolation seen in nearly all global SST records and reflects the high thermal inertia of water. The average range of the annual cycle (ACR) of the Guam SST is 1.97°C, and the ACR of the Gabgab coral Sr/Ca is 0.084 mmol/mol. The equivalence in Equation (2) is thus used hereafter to normalize and to examine the variability of the SST and Sr/Ca time series:

$$0.084\text{mmol/mol} = 1.97^{\circ}\text{C} \tag{2}$$

The following analyses of the long-term trend and of interannual and interdecadal variations make use of the corresponding Sr/Ca and SST ACR, whereby variations in the Sr/Ca time series and the SST time series may be normalized by their respective ACRs.

Long-Term Trends

After the assignment of years to the coral banding time series, the proxy results were compared with the Guam historical record of air temperature, SST, and the indices of El Niño and the PDO. As previously noted, the chosen historical record of SST for Guam was the Hadley Centre public SST data set (version 3). The linear trend of the raw SST from 1960 to 2010 is +0.12°C per decade, and the linear trend of the raw interpolated Sr/Ca is –0.0093 mmol/mol per decade (Figure 12). Normalized to their respective ACRs, the trend of SST is +0.06 ACR per decade, and the trend of Sr/Ca is –0.11 ACR per decade, both trends being indicative of warming. Normalized to the ACR, the long-term trend of the coral Sr/Ca [and its imputed magnitude of warming, using Equation (2)] is roughly double the trend of SST. The linear trends of the AAFB maximum, minimum, and average temperatures over the course of the period of record are +0.23°C, +0.15°C, and +0.07°C per decade, respectively. The long-term temperature trend implied by the Sr/Ca trend of –0.0093 mmol/mol per decade (*i.e*. +0.22°C) is thus closer to the trend of the AAFB maximum temperature than to the trends of the SST (Figure 13) or the AAFB average and minimum temperatures.

Interannual Variation and ENSO

ENSO effects span the globe, with notable modulation of many important weather features far from its core region of strong influence in the tropical Pacific, such as the character of the Atlantic hurricane season, the strength and timing of the Indian monsoon, and the amount of rainfall in NE Brazil (Ropelewski and Halpert, 1987). An ENSO signal has been

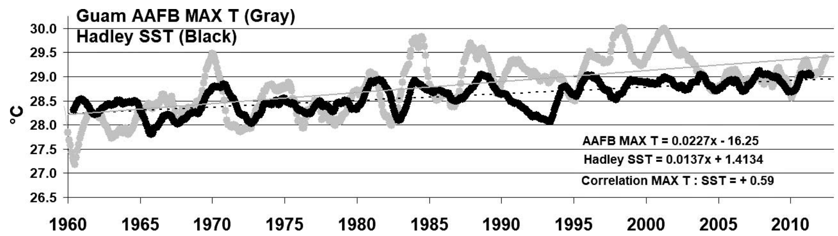

Figure 13. AAFB monthly average maximum air temperature (MAX T, gray) compared with Hadley SST (black). Plotted values are 12-mo moving averages of the respective monthly time series. Linear trend lines are included. The correlation value of the two time series is +0.59. Note that the MAX T linear trend is 165% greater than that of the SST. As discussed in the manuscript, there is some indication that the linear trend of the Sr/Ca proxy temperature more closely tracks that of the MAX T.

retrieved from coral cores across the Pacific, including from the Coral Sea (Calvo *et al.*, 2006), New Caledonia (Ourbak *et al.*, 2006), and even as far afield as the SW Atlantic (Evangelista *et al.*, 2007). Closer to the Gabgab study, an ENSO signal has been retrieved from a coral $\delta^{18}O$ time series near Guam (Asami *et al.*, 2005) and at Palau (Osborne *et al.*, 2014).

To more clearly reveal the interannual variability of the time series of the SST and of the Sr/Ca, a 12-month moving average was applied to each (Figure 12). The large interannual variations in the two time series are clearly related. (The simultaneous correlation value was –0.64.) That all the weather elements on Guam (*e.g.*, rainfall, SST, sea level, air temperature, and typhoon distribution) undergo large interannual variations that are dominated by ENSO (*cf.* Lander, 1994a) suggests the next step would be to compare the Sr/Ca time series to the Oceanic Niño Index, which is the operational ENSO index used by the National Oceanographic and Atmospheric Administration (NOAA) Climate Prediction Center (CPC, 2016). Although a plot of the raw Sr/Ca data against the raw ENSO index (Figure 14a) does not manifest an obvious correlation, application of a 12-month moving average to the Sr/Ca time series reveals some prominent peaks and troughs coinciding with peaks and troughs of the ENSO index (Figure 14b). A sixth-order polynomial fit to the Sr/Ca series (red line on Figure 14b) captures a longer period interdecadal fluctuation present in the Sr/Ca time series that is not apparent in the ENSO index series. Removing this interdecadal signal (the red line) by a simple subtraction from the smoothed Sr/Ca time series visibly strengthens the obvious correlation (Figure 14c) between the time series of Sr/Ca and the ENSO index (raw correlation is +0.47, $p < 0.01$).

Interdecadal Variation

Looking back at Figure 14b, it is clear that the Sr/Ca time series possesses a long-term fluctuation that is not present in the ENSO signal. In this figure, it can be seen that for roughly the 15-year period 1960 through 1975, the Sr/Ca time series rides mostly high above the plot of the ENSO index. Thereafter, for another 15-year period (*ca.* 1978–1992), the plot of the time series of Sr/Ca rides mostly below the ENSO time series. From 1992 through the end of the Sr/Ca time series in 2010, the magnitude of the long-term fluctuation is subdued, as captured by the sixth-order polynomial fit to the Sr/Ca time series. The peak-to-trough range of the interdecadal cycle, as represented by the sixth-order curve, is roughly equivalent to the magnitude of the interannual fluctuations. Whereas the roughly 3-year-period of sharp interannual fluctuations was earlier shown to correspond to the ENSO signal, it is suggested that the longer interannual fluctuation present in the Sr/Ca time series (but not in the ENSO time series) is a manifestation of the PDO.

With some additional smoothing (*i.e.* a 36-month moving average rather than a 12-month moving average) applied to the raw Sr/Ca time series to remove the sharp peaks and troughs of the interannual variability (shown earlier to correspond to the ENSO signal), there yet remains a large-amplitude interdecadal fluctuation that has undergone roughly two complete cycles over the course of the 50-year (*i.e.* 1960–2010) record (Figure 15). Also, in Figure 15, the PDO index (with a 12-month moving average applied) is overlain on the Sr/Ca time series. As was earlier—and again here—done to the Sr/Ca time series, a sixth-order polynomial was also fit to the time series of the PDO. It is clear that the peaks and troughs of the interdecadal variability in the Sr/Ca time series share some common patterns with the peaks and troughs of the PDO index, particularly during the first 35 years of the record when a coherent long-period fluctuation (highlighted by the sixth-order polynomials) is present in both time series. Published determinations of the long-term phases of the PDO show a cool (negative) phase during 1947 through 1976, transitioning to a warm (positive) phase from 1977 through 1999. After 1999, large shorter-term variations began to dominate the PDO. Note that the phase transition year of 1976 is precisely contained in each time series.

The PDO signal has been found in other coral cores in the Pacific basin and even in the Indian Ocean. An informative treatment of the pan-Pacific distribution of PDO retrievals in coral proxies is found in Evans *et al.* (2001). Coral proxy retrieval of the PDO signal has been reported in several locations in the Pacific Ocean: the South China Sea (Deng *et al.*, 2013), near Japan (Felis *et al.*, 2010), at Rarotonga (South Pacific) (Dima *et al.*, 2005; Linsley, Wellington, and Schrag, 2000; Linsley *et al.*, 2015; Nurhati, Cobb, and Di Lorenzo, 2011), and in the Line Islands (south of Hawaii) (Nurhati, Cobb, and Di Lorenzo, 2011). The recovery of a PDO signal is also reported in the Indian Ocean (Crueger, Zinke, and Pfeiffer, 2009; Pfeiffer *et al.*, 2009). The PDO signal found in the Indian Ocean by Pfeiffer *et al.* (2009) is reproduced in Figure 15b for

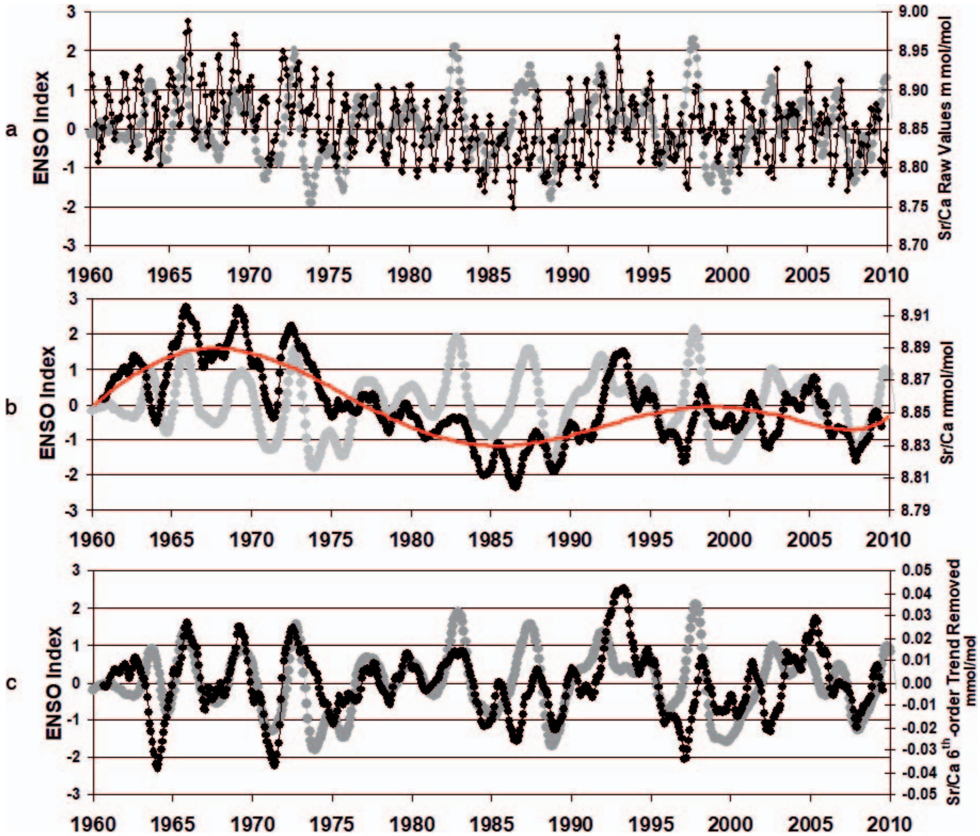

Figure 14. (a) The interpolated Gabgab Sr/Ca time series overlaid on a time series of the NOAA Climate Prediction Center's Operational Niño Index (ONI). The smaller black dots are the values of Sr/Ca and the larger gray dots are the values of the ONI. It is not apparent to the eye that there is a strong relationship between the ENSO index and the raw Sr/Ca time series. (b) The same data used to make panel (a), but with a 12-mo moving average applied to the Sr/Ca raw data. Once again, the interpolated Gabgab Sr/Ca time series is overlaid on a time series of the NOAA Climate Prediction Center's ONI. The smaller black dots are the values of Sr/Ca and the larger gray dots are the values of the ONI. The red line is a best fit sixth-order polynomial applied to the Sr/Ca data to highlight the obvious interdecadal rise and fall, which is not apparent in the ENSO Index. (c) The only difference in this chart from panel (b) is the removal (by direct subtraction) of the sixth-order polynomial in Figure 15b from the Sr/Ca time series. When this is done, there is a very obvious relationship between the Sr/Ca time series and ENSO. As in panels (a) and (b), the interpolated Gabgab Sr/Ca time series is overlaid on a time series of the NOAA Climate Prediction Center's ONI. The smaller black dots are the values of Sr/Ca and the larger gray dots are the values of the ONI. The strength of the ENSO signal in the Sr/Ca time series is much easier to perceive. The r-value of the cross-correlation between these two time series is +0.47.

comparison with the PDO signal found in this study. Both studies capture the 1976 phase shift. The importance of the 1976 phase shift of the PDO in identifying its presence in coral proxies is discussed in Liu *et al*. (2008). One possible mechanism (terrestrial runoff) for PDO signal capture by corals is discussed in Rodriguez-Ramirez *et al*. (2014).

Lastly, the Gabgab Sr/Ca time series (with only the annual cycle removed) is placed into its context of the longer available historical record of the PDO and of the 213-year δ^{18}O time series obtained by Asami *et al*. (2005) (Figure 16) from a coral in open water at Double Reef on Guam's NW coast (Figure 1b). Asami *et al*. (2005) claim to have captured historic and prehistoric ENSO variation in their δ^{18}O time series, as well as longer period fluctuations that they label as "warm and dry" and "cool and wet." In the 40-year period of the Sr/Ca time series overlap, with their longer δ^{18}O record and the longer PDO record, the same climatic influences appear. The results of this study thus provide independent confirmation of the results of Asami *et al*. (2005) and enhanced confidence in applications of both the δ^{18}O and Sr/Ca proxies for future Guam paleoclimate reconstruction.

DISCUSSION

This section discusses the fidelity of instrumental records to which the Sr/Ca record was compared, the Gabgab coral Sr/Ca record of ENSO and PDO, and the influence of harbor environmental conditions.

Fidelity of Instrumental Records to Which the Sr/Ca Record Was Compared

Comparison of proxy signals with meteorological records is only as valid as the records themselves. Official records of local climate data proved to be more limited and fraught with deficiencies than is commonly recognized. The comparisons reported here are therefore tempered by an acknowledgment and examination of the limitations of the extant climatic records and an explanation of how the data sets used in this

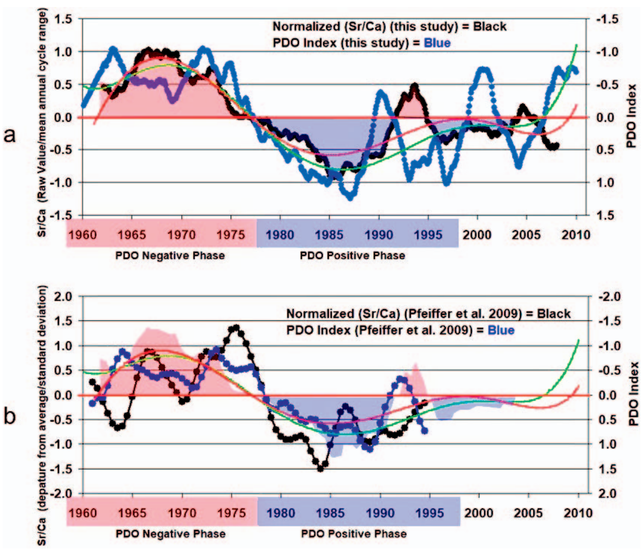

Figure 15. (a) The time series of the PDO index *vs*. the time series of the Gabgab Sr/Ca. Both time series have had a 3-y moving average applied to dampen the ENSO variability. The Sr/Ca time series values are normalized with respect to the average range of the annual cycle (0.084 mmol/mol). A sixth-order polynomial (red for Sr/Ca and green for the PDO) has been fit to each time series to emphasize the coherence of the decadal variability in each record. Phase shifts of the PDO are indicated by color shading along the *x* axis. (b) The time series of Sr/Ca found by Pfeiffer *et al*. (2009) from a composite of five coral cores in the tropical Indian Ocean. Values plotted are departures from the time-series average divided by the standard deviation (as per their methodology). Their PDO index is indicated by the blue dots, and their coral Sr/Ca is indicated by the black dots. The shading and sixth-order polynomials are carried over from panel (a) to help illustrate the shared behavior.

study were thus composed. The first problem is the low spatial resolution of the standard SST data and the dearth of long-term local data for any given location. This study (like others, including Asami *et al*., 2005) relied on a publicly available SST data set (with data at a grid scale twice the length of Guam). It was not immediately certain that publicly available SST data sets would provide information relevant to variability at small scales, especially for a point in a shallow-water site of a single harbor on the west side of Guam. However, several months of SST measurements collected at the Gabgab site tracked the Hadley SST remarkably well (Figure 6). Other problems that became manifest were errors in the officially available climate records, even from Guam's best long-term stations. Official climate data for Guam available online from the NCDC suffer from losses of data that are recoverable from local sources. For example, the NCDC record of daily data for AAFB suffers from 2.7% missing data, in contrast to the local AAFB record, which is more than 99.9% complete. Another problem was the discovery that the NOAA long-term record for the Weather Service Forecast Office at the Guam International Airport is a concatenation of data from two separate stations that are several miles apart, and with substantial differences in temperature and rainfall. Given the authors' familiarity with the local climate, access to original complete data sets, knowledge of missing typhoon data, knowledge of errors in the data, and access to supplemental unofficial climate data, the authors are confident that they have assembled a better climate record than can be obtained off the shelf and are commensurately confident in the comparisons reported herein.

Gabgab Coral Sr/Ca Record of ENSO and PDO

As noted above, the Gabgab Sr/Ca time series captured four prominent observed behaviors of the local climate: (1) an annual cycle, (2) a long-term trend (*i.e*. SST and air temperature increase), (3) substantial interannual variation (*i.e*. ENSO), and (4) substantial interdecadal variation (*i.e*. PDO). If nothing else, the annual cycle of SST was anticipated to show prominently in the Gabgab Sr/Ca time series, followed in prominence by a long-term warming trend and, to a lesser extent, an ENSO signal. It was somewhat unexpected that the PDO appears to have been captured so well in the coral record. The PDO has its strongest signal in the midlatitudes of the North Pacific but does have a nonnegligible signal in the tropics with a similar spatial pattern as ENSO, albeit with some longer periodicity (*i.e*. whereas ENSO is primarily interannual, the PDO is strongly interdecadal). The PDO certainly contributes to variability of the local climate—even if only by, or perhaps primarily through, its possible modulation of ENSO: The climate signal of El Niño is likely to be stronger when the PDO is highly positive; conversely, the climate signal of La Niña will be stronger when the PDO is highly negative (Gershunov and

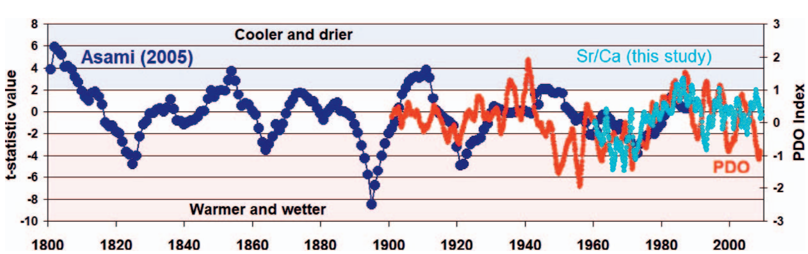

Figure 16. An overlay of three time series: (dark blue) Guam δ^{18}O record of Asami *et al*. (2005); (red) PDO index; (light blue) Gabgab Sr/Ca time series. The time series of the PDO index and of the Sr/Ca values have been smoothed with 12-mo moving average. Plotted values are the *t*-statistic (left-hand scale) taken directly from a plot of this in the Asami *et al*. (2005) paper and the PDO index (right-hand scale). The Gabgab Sr/Ca time series has been scaled for visual comparison to the other time series. The attribution of the climate condition (cooler and drier *vs*. warmer and wetter) is labeled as per the figure of Asami *et al*. (2005).

Barnett, 1998). The results of the comparison of the Gabgab Sr/Ca time series with local observed climate far exceeded the initial expectations and goals of this study.

Interdecadal Modulation of ENSO Teleconnections

The 50-year Gabgab proxy record recovered instrumentally documented signals of the larger Pacific climate fluctuations of ENSO and PDO and a long-term trend that is consistent with that of the historical data. The authors do not know at this time why the proxy captures the large-scale climate signals so well. Perhaps it is through the relation of ENSO and PDO to the local SST. However, ENSO and PDO also affect many other local climatic elements, such as hours of direct sunlight (modulated by cloudiness) and changes in sea level. Considering merely the sea level, for example, the difference in monthly mean sea level between the peak of a strong El Niño and the peak of a strong La Niña is about 0.5 m (nearly 2 feet). This is on par with Guam's mean daily tidal range of 0.75 m (2.6 feet). At its subsurface depth of merely 2 m, it is possible that a change of mean sea level on the order 25% of the mean water depth might have some influence on the Gabgab coral through modulation of sunlight, water temperature, or other links.

Influence of Harbor Environmental Conditions

The enclosed harbor setting of the Gabgab site contrasts with the open coastal water setting of the Double Reef site (Figure 1b) from which Asami *et al*. (2004, 2005) collected their sample. Prouty *et al*. (2014) collected coral cores from Apra Harbor, just south of the Luminao Reef, almost exactly opposite Gabgab Beach. They noted that salinity measurements by Storlazzi, Presto, and Logan (2009) indicated freshwater input into Apra Harbor but concluded that most sediment is likely deposited in the inner harbor (Figure 1c) so that sites in the outer harbor would not be strongly affected by terrigenous sediment. The study reported here thus sought to examine the validity of this assumption while also examining the broader question of whether coral from enclosed, nearshore sites might produce useful climate records even though water chemistry might differ from pristine, open-ocean conditions.

For the reconstruction of historical SST, these questions are important because the utility of the Sr/Ca-SST coral proxy is based on the assumption that seawater Sr is constant, primarily as a function of its long residence time (>4 Ma) relative to oceanic mixing (10^3 y; Broecker 1963) and its conservative nature (*e.g*., homogeneous distribution spatially). However, the fidelity of the coral-derived Sr/Ca thermometry can be compromised by several factors, including variable calcification and extension rates (*e.g*., Cohen *et al*., 2004; de Villiers, Shen, and Nelson, 1994), variability in seawater Sr/Ca composition (*e.g*., de Villiers 1999; Shen *et al*., 1996; Sun *et al*., 2005), and interspecies differences (see DeLong *et al*., 2011) that can influence the Sr/Ca-SST calibration. In some cases, these factors can be addressed by accounting for growth rate (*e.g*., Goodkin, Hughen, and Cohen, 2007; Saenger *et al*., 2008), employing microsampling (see summary by Jones *et al*., 2009) and avoiding sampling sites sensitive to riverine or submarine ground discharge that can alter the seawater composition (DeLong *et al*., 2011, 2014; Flannery and Poore, 2013; Maupin, Quinn, and Halley, 2008). Understanding these effects and minimizing their influence whenever possible will increase the robustness of the coral Sr/Ca proxy.

Therefore, a robust transfer function relating Sr/Ca to SST for the Gabgab coral was unexpected. The most significant outcomes of this study were that (1) despite the site being in a nonoptimal environment, the transfer function [Equation (1)] was nevertheless consistent with an analogous previous result from the western Pacific using the same species, notably Correge (2006), and that (2) whatever the quality of the Sr/Ca-SST transfer function, the Sr/Ca time series reflected ENSO and PDO histories with remarkable fidelity. If the fidelity of the Sr/Ca time series to the interdecadal climate signals simply reflects correlation with the SST at the site, then the Sr/Ca-SST transfer function is at least sufficiently robust to have captured variations in site SST that correlate with the ENSO and PDO signals. If, on the other hand, the validity of the Sr/Ca record as proxy for SST has been compromised by geochemical variations at the site, the fidelity of the Sr/Ca time series to the ENSO and PDO signals indicates that the Sr/Ca record must be responding to other environmental variables besides SST that are correlated with ENSO and PDO, such as perhaps sea-level fluctuations, as speculated in the previous section.

As mentioned above, seawater Sr/Ca ratios at the Gabgab site ranged from 8.90 to 9.36 mmol/mol (Table 2 and Figure 5b), suggesting that seawater Sr/Ca in Apra Harbor does not demonstrate the conservative behavior typically assumed in paleoceanographic studies. The standard deviation of $\pm$0.14 mmol/mol could in principle have thus influenced the coral-derived thermometry by as much as 7°C by Equation (1). It has been shown that exogenous Sr in the nearshore environment can complicate the utility of the coral Sr/Ca-SST proxy (*e.g*., Reich *et al*., 2013). However, the Sr concentration at the Gabgab site, 7.59 $\pm$ 0.21 ppm, is not enriched; instead the average Ca concentration, 383.07 $\pm$ 7.52 ppm, suggests that lower Ca concentrations may be responsible for elevated seawater Sr/Ca ratios. However, given that Ca is the major element in coral skeletons, variance in seawater Ca should not significantly affect Ca uptake by corals. The most probable source of Ba to the nearshore environment is terrestrial runoff. As described in Prouty *et al*. (2014), river Ba concentrations were elevated relative to seawater Ba concentrations (*i.e*. 193 ppb *vs*. 92 ppb). The Ba concentration from Prouty *et al*. (2014) is within the range present for Apra Harbor from this study: 86.31 $\pm$ 15.88 ppb.

Finally, the authors note that in a recent work postdating this study, four additional coral colonies from Guam were cored and analyzed (McCutcheon *et al*., 2014, 2015), including one from the north side of Apra Harbor, opposite the Gabgab site. Only two of the four cores showed significant correlation with SST. Coral growth parameters could not explain differences in the individual coral Sr/Ca records. Sr/Ca proxy studies, including this one, should be interpreted with such considerations in mind. Nevertheless, the recovery of local historical climate from the Gabgab coral Sr/Ca record indicates that coral growing in such conditions (including, but not limited to, restrictions to the free flow of seawater and some direct stream influx) can yield a reliable Sr/Ca proxy record of the observed long-term trend of rising temperature, El Niño events and the local manifestations of PDO phase shifts. Additionally, benchmark climate signals may be captured, even in the absence of a reliable proxy-SST transfer function.

CONCLUSIONS

In summary, a 50-year monthly Sr/Ca time series was obtained from a core drilled in a 60-year-old colony of *P. lutea* located near the margin of the reef at Gabgab Beach, Apra Harbor, Guam, where the top of the coral head is covered by about 2 m of water (Figure 3). Four observations stand out. First, the Gabgab Sr/Ca time series provides a reliable record of local SST (Figure 12). Second, time series of seawater $\delta^{18}O$, pH (Figure 5), and cations (Table 2 and Figure 5) show evidence of freshwater input from direct rainfall or stream discharge into the harbor. An anomalously higher mean and variable concentration of Ba suggest the presence of river-borne, fine-grained terrigenous sediment, but the fidelity of the Sr/Ca record appears not to have been adversely affected by riverine freshwater discharge into the harbor. Third, the Gabgab Sr/Ca time series shows convincing evidence of variability related to ENSO and PDO (Figures 14 and 15) and is consistent with the interdecadal variability of the $\delta^{18}O$ record found by Asami *et al*. (2004, 2005) in a deeper water coral in an open-water coastal location (Figure 16). Finally, the results of this project—in particular, the consistency of the Gabgab coral Sr/Ca SST signal with instrumental records and with the $\delta^{18}O$ record obtained by Asami *et al*. (2004, 2005)—indicate that a reliable Sr/Ca record can be obtained from an accessible nearshore, shallow-water coral in other than pristine conditions—in this case, a busy harbor with ship traffic and freshwater input from streams.

ACKNOWLEDGMENTS

Work on this project was funded by the U.S. Geological Survey (grant 11HQPA 30002); the Pacific ENSO Application Center (grant 65A283); the Guam Hydrologic Survey at the Water & Environmental Research Institute of the Western Pacific, University of Guam; and the Richard F. Taitano Micronesian Area Research Center at the University of Guam. The authors thank U.S. Naval Base, Guam, for access to Gabgab Beach and the Guam Department of Agriculture for the permit for coral sampling. Tetsuya Endo, Celery Corporation, Japan, designed and built the unique underwater drill used for this study. Jason Miller, University of Guam Marine Laboratory, captained the boat and assisted in the drilling. The authors especially express their appreciation to colleagues at the University of Texas-Austin: Terry Quinn generously provided advice and support for the analyses, including the use of his laboratory. Fred Taylor provided valuable advice on underwater drilling and use of his laboratory for x-rays. Chris Maupin assisted in preparation of the coral slabs. Megan Gorman generously assisted with operation of laboratory equipment and provided timely assistance in preparing and correcting the time-series data. Thanks also to Kelly Hereid and Kaustaubh Thirumalai for laboratory assistance. The authors also express their appreciation to Yusuke Yokoyama and the Department of Science, University of Tokyo, for providing the means for the lead author to travel to visit and work directly on the manuscript with co-authors at the University of Guam. Colleagues at the University of Guam also provided generous assistance: Jennifer Cruz provided training and assistance in the application of laboratory equipment in the WERI Water Quality Laboratory. Vivianna Bendixson provided field assistance on follow-up site surveys. Ben Hardt contributed advice and assistance in some of the statistical analyses and in the preparation of the WERI technical report from which this paper proceeded. Maria Kottermair graciously built the maps. Nathan Habana provided GIS analyses of Apra Harbor hydrology. Adam Johnson, USGS Pacific Island Water Science Center, Honolulu, generously provided water budget data for Apra Harbor and the adjacent watershed.

LITERATURE CITED

Asami, R.; Yamada, T.; Iryu, Y.; Meyer, C.P.; Quinn, T.M., and Paulay, G., 2004. Carbon and oxygen isotopic composition of a Guam coral and their relationships to environmental variables in the western Pacific. *Palaeogeography, Palaeoclimatology, Palaeoecology*, 212, 1–22.

Asami, R.; Yamada, T.; Iryu, Y.; Quinn, T.M.; Meyer, C.P., and Paulay, G., 2005. Interannual and decadal variability of the western Pacific sea surface condition for the years 1787–2000: Reconstruction based on stable isotope record from a Guam coral. *Journal of Geophysical Research*, 110(C05018). doi:10.1029/2004JC002555

Ashok, K.; Behera, S.K.; Rao, S.A.; Weng, H., and Yamagata, T., 2007. El Nino Modoki and its possible teleconnection. *Journal of Geophysical Research*, 112(C11007). doi:10.1029/2006JC003798

Atkinson, M.J.; Carson, B., and Crow, G.L., 1995. Coral growth in high-nutrient, low-pH seawater: A case study of corals cultured at Waikiki aquarium Honolulu, Hawaii. *Coral Reefs*, 14(4), 215–223.

Bell, T.; Endo, T.; Jenson, J.W.; Bell, R., and Lander, M.A., 2011. *Pneumatic Underwater Drill for Extracting Coral Cores*. Mangilao, Guam: Water and Environmental Research Institute of the Western Pacific, University of Guam, *WERI Technical Report No. 135*, 18p.

Bell, T.; Iguchi, A.; Suzuki, A.; Seki, A., and Yokoyama, Y., 2018. Testing possible relationships between *Acropora digitifera* genes, seawater chemistry and skeletal elements. *Geochemical Journal*, 52(3), 263–272. doi.org/10.2343/geochemj.2.0511

Bell, T.; Lander, M.A.; Jenson, J.W.; Randall, R.H.; Partin, J.W., and Hardt, B.F., 2012. *Coral and Speleothem* in situ *Monitoring and Geochemical Analysis. Guam, Mariana Islands, USA*. Mangilao, Guam: Water and Environmental Research Institute of the Western Pacific, University of Guam, *WERI Technical Report No. 136*, 62p.

Bell, T.; Nishida, K.; Ishikawa, K.; Suzuki, A.; Nakamura, T.; Sakai, K.; Ohno, Y.; Iguchi, A., and Yokoyama, Y., 2017. Temperature-controlled culture experiments with primary polyps of coral *Acropora digitifera*: Calcification rate variations and skeletal Sr/Ca, Mg/Ca, and Na/Ca ratios. *Palaeogeography, Palaeoclimatology, Palaeoecology*, 484, 129–135. doi.org/10.1016/j.palaeo.2017.03.016

Broecker, W.S., 1963. A preliminary evaluation of uranium series inequilibrium as a tool for absolute age measurement on marine carbonates. *Journal of Geophysical Research*, 68(9), 2817–2834. doi:10.1029/JZ068i009p02817

Brown, G.M.; Holland, J.G.; Sigurdsson, H.; Tomblin, J.F., and Arculus, R.J., 1977. Geochemistry of the Lesser Antilles volcanic island arc. *Geochimica et Cosmochimica Acta*, 41(6), 785–801.

Calvo, E.; Marshall, J.F.; Pelejero, C.; McCulloch, M.T.; Gagan, M.K., and Lough, J.M., 2006. Interdecadal climate variability in the Coral Sea since 1708 A.D. *Palaeogeography, Palaeoclimatology, Palaeoecology*, 248(1–2), 190–201.

Cohen, A.L.; Smith, S.R.; McCartney, M.S., and van Etten, J., 2004. How brain corals record climate: An integration of skeletal structure, growth and chemistry of *Diploria labyrinthiformis* from Bermuda. *Marine Ecology Progress Series,* 271, 147–158.

Correge, T., 2006. Sea surface temperature and salinity reconstruction from coral geochemical tracers. *Paleoceanography, Paleoclimatology, Paleoecology*, 232(2–4), 408–428.

CPC (Climate Prediction Center), 2016. *Cold & Warm Episodes by Season*. http://www.cpc.ncep.noaa.gov/products/analysis_monitoring/ensostuff/ensoyears.shtml.

Craig, H., 1961. Isotopic variations in meteoric waters. *Science*, 133(3465), 1702–1703.

Crueger, T.; Zinke, J., and Pfeiffer, M., 2009. Patterns of Pacific decadal variability recorded by Indian Ocean corals. *International Journal of Earth Science*, 98, 41–52.

de Villiers, S., 1999. Seawater strontium and Sr/Ca variability in the Atlantic and Pacific oceans. *Earth and Planetary Science Letters*, 171, 623–634.

de Villiers, S.; Shen, G.T., and Nelson, B.K., 1994. The Sr/Ca temperature relationship in coralline aragonite: Influence of variability in Sr/Ca seawater and skeletal growth parameters. *Geochemica et Cosmochemica Acta*, 58(4), 197–208.

Dean, J.M. and Kemp, A.E.S., 2004. A 2100 year BP record of the Pacific Decadal Oscillation, El Niño Southern Oscillation and Quasi-Biennial Oscillation in marine production and fluvial input from Saanich Inlet, British Columbia. *Palaeogeography, Palaeoclimatology, Palaeoecology*, 213(3–4), 207–229.

DeLong, K.L.; Flannery, J.A.; Maupin, C.R.; Poore, R.Z., and Quinn, T.M., 2011. A coral Sr/Ca calibration and replication study of two massive corals from the Gulf of Mexico. *Palaeogeography, Palaeoclimatology, Palaeoecology*, 307(1–4), 117–128.

DeLong, K.L.; Flannery, J.A.; Poore, R.Z.; Quinn, T.M.; Maupin, C.R.; Lin, K., and Chen, C, 2014. A reconstruction of sea surface temperature variability in the southeastern Gulf of Mexico from 1734 to 2008 C.E. using cross-dated Sr/Ca records from the coral *Siderastrea sidera*. *Paleoceanography,* 29(5), 403–422. doi:10.1002/2013PA002524

Deng, W.; Wei, G.; Xie, L.; Ke, T.; Wang, Z.; Zeng, T., and Liu, Y., 2013. Variations in the Pacific Decadal Oscillation since 1853 in a coral record from the northern South China Sea. *Journal of Geophysical Research*, 118(5), 2358–2366.

Dima, M.; Felis, T.; Lohmann, G., and Rimbu, N., 2005. Distinct modes of bidecadal and multidecadal variability in a climate reconstruction of the last centuries from a South Pacific coral. *Climate Dynamics,* 25(2–3), 329–336.

Evangelista, H.; Godiva, D.; Sifeddine, A.; Leao, Z.M.A.N.; Kikuchi, R.K.P., and Le Cornec, F., 2007. Evidences linking ENSO and coral growth in the Southwestern–South Atlantic. *Climate Dynamics*, 29(7–8), 869–880.

Evans, M.N.; Cane, M.A.; Schrag, D.P.; Kaplan, A.; Linsley, B.K.; Villalba, R., and Wellington, G.M., 2001. Support for tropically-driven Pacific decadal variability based on paleoproxy evidence. *Geophysical Research Letters*, 28(19), 3689–3692.

Felis, T.; Suzuki, A.; Kuhnert, H.; Rimbu, N., and Kawahata, H., 2010. Pacific Decadal Oscillation documented in a coral record of North Pacific winter temperature since 1873. *Geophysical Research Letters*, 37(14), L14605.

Flannery, J.A. and Poore, R.Z., 2013. Sr/Ca proxy sea-surface temperature reconstructions from Modern and Holocene *Montastrea faveoolata* specimens from the Dry Tortugas National Park, Florida, U.S.A. *In:* Brock, J.C.; Barras, J.A., and Williams, S.J. (eds.), *Understanding and Predicting Change in the Coastal Ecosystems of the Northern Gulf of Mexico*. *Journal of Coastal Research*, Special Issue No. 63, pp. 20–31.

Francis, R.C. and Hare, S.R., 1994. Decadal-scale regime shifts in the large marine ecosystems of the North-east Pacific: A case for historical science. *Fisheries Oceanography*, 3(4), 279–291.

Gershunov, A. and Barnett, T.P., 1998. Interdecadal Modulation of ENSO Teleconnections. *Bulletin of the American Meteorological Society*, 79(12), 2715–2725.

Glantz, M.H.; Katz, R.W., and Nicholls, N., 1991. *Teleconnections Linking Worldwide Climate Anomalies*. Cambridge: Cambridge University Press, 548p.

Goodkin, N.F.; Hughen, K.A., and Cohen, A.L., 2007. A multicoral calibration method to approximate a universal equation relating Sr/Ca and growth rate to sea surface temperature. *Paleoceanography*, 22(1), PA1214. doi:10.1029/2006PA001312

Johnson, A.G., 2012. *A water-budget model and estimates of groundwater recharge for Guam*. Reston, Virginia: U.S. Geological Survey, *Scientific Investigations Report 2012–5028*, 53p.

Jones, P.D.; Briffa, K.R.; Osborn, T.J.; Lough, J.M.; van Ommen, T.D.; Vinther, B.M.; Luterbacher, J.; Wahl, E.R.; Zwiers, F.W.; Mann, M.E.; Schmidt, G.A.; Ammann, C.M.; Buckley, B.M.; Cobb, K.M.; Esper, J.; Goosse, H.; Graham, N.; Jansen, E.; Kiefer, T.; Kull, C.; Kuttel, M.; Mosley-Thompson, E.; Overpeck, J.T.; Riedwyl, N.; Schulz, M.; Tudhope, A.W.; Villalba, R.; Wanner, H.; Wolff, E., and Xoplaki, E., 2009. High-resolution palaeoclimatology of the last millennium: A review of current status and future prospects. *The Holocene,* 19, 3–49.

Lander, M.A., 1994a. An exploratory analysis of the relationship between tropical storm formation in the western North Pacific and ENSO. *Monthly Weather Review*, 122(4), 636–651.

Lander, M.A., 1994b. *Meteorological Factors Associated with Drought on Guam*. Mangilao, Guam: Water and Environmental Research Institute of the Western Pacific, University of Guam, *WERI Technical Report No. 75*, 39p.

Linsley, B.K.; Wellington, G.M., and Schrag, D.P., 2000. Decadal sea surface temperature variability in the subtropical South Pacific from 1726 to 1997 A.D. *Science*, 290(5494), 1145–1148.

Linsley, B.K.; Wu, H.C.; Dassie, E.P., and Schrag, D.P., 2015. Decadal chages in South Pacific sea surface temperatures and the relationship to the Pacific Decadal Oscillation and upper ocean heat content. *Geophysical Research Letters*, 42, 2358–2366.

Liu, Y.; Peng, Z.; Chen, T.; Wei, G.; Sun, W.; Sun, R.; He, J.; Liu, G.; Chou, C.-L., and Zartman, R.E., 2008. The decline of winter monsoon velocity in the South China Sea through the 20th century: Evidence from the Sr/Ca records in corals. *Global and Planetary Change*, 63(1), 79–85.

Mantua, N.J.; Hare, S.R.; Zhang, Y.; Wallace, J.M., and Francis, R.C., 1997. A Pacific interdecadal climate oscillation with impacts on salmon production. *Bulletin of the American Meteorological Society*, 78(6), 1069–1079.

Marubini, F. and Davies, P.S., 1996. Nitrate increases zooxanthellae population density and reduces skeletogenesis in corals. *Marine Biology*, 127(2), 319–328.

Maupin, C.R.; Quinn, T.M., and Halley, R.B., 2008. Extracting a climate signal from the skeletal geochemistry of the Caribbean coral *Siderastrea siderea*. *Geochemistry, Geophysics, Geosystems*, 12, Q12012. doi:10.29/2008GC002106

McCutcheon, A.L.; Raymundo, L.; Jenson, J.W.; Lander, M.A., and Randall, R.H., 2014. Testing the Sr/Ca proxy for sea-surface temperature reconstruction in the coral *Porites lutea*, Guam, Micronesia. *Proceedings of Ocean Sciences Meeting* (Honolulu, Hawaii, Association for the Sciences of Limnology and Oceanography, The Oceanography Society, and the American Geophysical Union).

McCutcheon, A.L.; Raymundo, L.J.; Jenson, J.W.; Prouty, N.G.; Lander, M.A., and Randall, R.H., 2015. *Testing the Strontium/Calcium Proxy for Sea Surface Temperature Reconstruction in the Coral* Porites lutea*, in Guam, Micronesia*. Mangilao, Guam: University of Guam Marine Laboratory and Water & Environmental Research Institute of the Western Pacific, *UOGML Technical Report 159, WERI Technical Report 152*, 87p.

Merrifield, M.A.; Thompson, P.R., and Lander, M.A., 2012. Multidecadal sea level anomalies and trends in the western tropical Pacific. *Geophysical Research Letters*, 39(13), L13602. doi:10.1029/2012GL052032

Messie, M. and Chavez, F., 2011. Global modes of sea surface temperature variability in relation to regional climate indices. *Journal of Climate*, 24(16), 4314–4334.

Mitsuguchi, T.; Dang, P.X.; Kitagawa, H.; Uchida, T., and Shibata, Y., 2008. Cral Sr/Ca and Mg/Ca records in Con Dao Island off the Mekong Delta: Assessment of their potential for monitoring ENSO and East Asian monsoon. *Global and Planetary Change*, 63(4), 341–352.

Montaggioni, L.F.; Le Cornc, F.; Correge, T., and Cabioch, G., 2006. Coral barium/calcium record of mid-Holocene upwelling activity in

New Caledonia, South-West Pacific. *Palaeogeography, Palaeoclimatology, Paleoecology*, 237(2–4), 436–455.

Moreau, M.; Correge, T.; Dassie, E.P., and Le Cornec, F., 2015. Evidence for the non-influence of salinity variability on the *Porites* coral Sr/Ca paleothermometer. *Climate of the Past*, 11, 523–532.

Newman, M.; Compo, G.P., and Alexander, M.A., 2003. ENSO-forced variability of the Pacific Decadal Oscillation. *Journal of Climate*, 16(23), 3853–3857.

Nurhati, I.S.; Cobb, K.M., and Di Lorenzo, E., 2011, Decadal-scale SST and salinity variations in the central tropical Pacific: Signatures of natural and anthropogenic climate change: *Journal of Climate*, 24, 3294–3308.

Osborne, M.C.; Dunbar, R.B.; Mucciarone, D.A.; Druffel, E., and Sanchez-Cabeza, J.-A., 2014. A 215-yr coral $d^{18}O$ time series from Palau records dynamics of the West Pacific Warm Pool following the end of the Little Ice Age. *Coral Reefs*, 33(3), 719–731.

Ourbak, T.; Correge, T.; Malaize, B.; Le Cornec, F.; Charlier, K., and Peypouquet, J.P., 2006. ENSO and interdecadal climate variability over the last century documented by geochemical records of two coral cores from the South West Pacific. *Advances in Geosciences*, 6, 23–27.

Paillard, D.; Labeyrie, L., and Yiou, P., 1996. Macintosh program performs time-series analysis. *EOS*, 77(39). doi:10.1029/96EO00259

Partin, J.W.; Jenson, J.W.; Banner, J.L.; Quinn, T.M.; Taylor, F.W.; Sinclair, D.; Hardt, B.F.; Lander, M.A.; Bell, T.; Miklavič, B.; Jocson, J.M.U., and Taboroši, D., 2012. Relationship between modern rainfall variability, cave dripwater and stalagmite geochemistry in Guam, USA. *Geochemisty, Geophysics, Geosystems*, 13(3), 1–17.

Pfeiffer, M.; Dullo, W.-C.; Zinke, J., and Garbe-Schonberg, D., 2009. Three monthly coral Sr/Ca records from the Chagos Achipelago covering the period of 1950–1995 A.D.: Reproducibility and implications for quantitative reconstructions of sea surface temperature variations. *International Journal of Earth Science*, 98, 53–66.

Pilson, M.E.Q., 2103. *An Introduction to the Chemistry of the Sea*. Cambridge: Cambridge University Press, 533p.

Prouty, N.G.; Storlazzi, C.D.; McCutcheon, A.L., and Jenson, J.W., 2014. Historic impact of watershed change and sedimentation to reefs along west-central Guam. *Coral Reefs*, 33(3), 733–749. doi 10.1007/s00338-00014-01166-x

Ramage, C.S., 1995. *Forecasters Guide to Tropical Meteorology—AWS TR 240 Updated*. Scott Air Force Base, Illinois, Air Weather Service, US Air Force Environmental Technical Applications Center, *AWS/TR-95-001*, 452p.

Reich, C.D.; Kuffner, I.B.; Hickey, T.D.; Morrison, J.M., and Flannery, J.A., 2013. *Complexity of Nearshore Strontium-to-Calcium Ratio Variability in a Core Sample of the Massive Coral* Siderastrea siderea *Obtained in Coral Bay, St. John, U.S. Virgin Islands*. Reston, Virginia: U.S. Geological Survey, *Open-File Report, 2013-1092*, 12p.

Rodriguez-Ramirez, A.; Grove, C.A.; Zinke, J.; Pandolfe, J.M., and Zhou, J.-X., 2014. Coral luminescence identifies the Pacific Decadal Oscillation as the primary driver of river runoff variability impacting the southern Great Barrier Reef. *PLoS ONE*, 9(1), e84305. https://doi.org/10.1371/journal.pone.0084305.

Ropelewski, C.F. and Halpert, M.S., 1987. Global and regional scale precipitation patterns associated with the El Niño/Southern Oscillation. *Monthly Weather Review,* 115(8), 1606–1626.

Sadler, J.C.; Lander, M.A.; Hori, A.M., and Oda, L.K., 1987. *Tropical Marine Climatic Atlas, Vol. II, Pacific Ocean*. Manoa, Hawaii: University of Hawaii, Department of Meteorology, *UHMET-87-02*, March 1987 (updated web and CD versions, March 2003).

Saenger, C.; Cohen, A.L.; Oppo, D.W., and Hubbard, D., 2008. Interpreting sea surface temperature from strontium/calcium ratios in *Montastrea* corals: Link with growth rate and implications for proxy reconstructions. *Palaeogeography, Palaeoclimatology, Palaeoecology*, 23(PA3102). doi:10.1029/2007PA001572

Shen, C.C.; Lee, T.; Chen, C.; Wang, C.; Dai, C., and Li, A., 1996. The calibration of D[Sr/Ca] versus sea surface temperature relationship for *Porites* corals. *Geochemica et Cosmochimica Acta*, 60(20), 3849–3858.

Shinjo, R.; Asami, R.; Huang, K.-F.; You, C.-F., and Iryu, Y., 2013. Ocean acidification trend in the tropical North Pacific since the mid-20th century reconstructed from a coral archive. *Marine Geology*, 342, 58–64.

Sinclair, D.; Banner, J.L.; Taylor, F.W.; Partin, J.W.; Jenson, J.W.; Mylroie, J.E.; Goddard, E.; Quinn, T.M.; Jocson, J.M.U., and Miklavič, B., 2012. Magnesium and strontium systematics in tropical speleothems from the western Pacific. *Chemical Geology*, 294–295, 1–17.

Sinclair, D.J.; Banner, J.L.; Taylor, F.W.; Quinn, T.M.; Jenson, J.W., and Mylroie, J.E., 2008. Deglacial climate dynamics in the western Pacific Ocean measured in a stalagmite from Guam. *Proceedings of the Goldschmidt Conference* (Vancouver, British Columbia), p. A870.

Smith, J.M.; Quinn, T.M.; Hemle, K.P., and Halley, R.B., 2006. Reproducibility of geochemical and climatic signals in the Atlantic coral *Montastraea faveolata*. *Paleoceanography*, 21(PA1010). doi:10.1029/2005PA001187

Smith, S.V.; Buddemeier, R.W.; Redalje, R.C., and Houck, J.E., 1979. Strontium-calcium thermometry in coral skeletons. *Science*, 204(4391), 404–406.

Storlazzi, C.D.; Presto, M.K., and Logan, J.B., 2009. *Coastal Circulation and Sediment Dynamics in War-in-the-Pacific National Historical Park, Guam: Measurements of Waves, Currents, Temperature, Salinity, and Turbidity, June 2007–January 2008*. Reston, Virginia: U.S. Geological Survey, *Open-File Report 2009-1195*, 79p.

Sun, Y.; Sun, M.; Lee, T., and Nie, B., 2005. Influence of seawater Sr content on coral Sr/Ca and Sr thermometry. *Coral Reefs*, 24, 23–29.

Swart, P.K.; Elderfield, H., and Greaves, M.J., 2002. A high-resolution calibration of Sr/Ca thermometry using the Caribbean coral *Montastrea annularis*. *Geochemistry Geophysics Geosystems*, 3(8402). doi 10.1029/2002GC000306

Taboroši, D.; Jenson, J.W., and Mylroie, J.E., 2005. Karst features of Guam, Mariana Islands. *Micronesica*, 38(1), 17–46.

USGS (U.S. Geological Survey), 2016. *USGS Coral Reef Project: Guam*. Santa Cruz, California: Pacific Coastal and Marine Science Center. http://coralreefs.wr.usgs.gov/guam.html.

Wang, B. and Ho, L., 2002. Rainy season of the Asian-Pacific monsoon. *Journal of Climate*, 15, 386–398.

Wang, S.; Huang, J.; He, Y., and Guan, Y., 2014. Combined effects of the Pacific Decadal Oscillation and El Niño–Southern Oscillation on global land dry-wet changes. *Scientific Reports* 4(6651). doi 10.1038/srep06651

Yan, X.-H.; Ho, C.-R.; Zheng, Q., and Klemas, V., 1992. Temperature and size variabilities of the western Pacific Warm Pool. *Science*, 258(5088), 1643–1645.